UNIVERSITY OF CALIFORNIA,

IRVINE

Flexural Behavior of Two-Way Sandwich Slabs

THESIS

submitted in partial satisfaction of the requirements
for the degree of

MASTER OF SCIENCE

in CIVIL ENGINEERING

by

JIVAN VILAS PACHPANDE

Thesis Committee:
Professor Ayman S. Mosallam, Chair
Associate Professor Farzin Zareian
Assistant Professor Mohammad Javad Abdolhosseini Qomi

2015

DEDICATION

It is with my deepest gratitude and warmest affection

that I dedicated this thesis to our Professor Dr. Ayman S. Mosallam

Who has been a constant source of Knowledge and Inspiration.

TABLE OF CONTENT

LIST OF FIGURES

LIST OF TABLES

ACKNOWLEDGMENTS

I would like to express the deepest appreciation to my committee chair, Professor Ayman S. Mosallam, who has the attitude and the substance of a genius: he continually and convincingly conveyed a spirit of adventure in regard to research and scholarship, and an excitement in regard to teaching. Without his guidance and persistent help this dissertation would not have been possible.

I would like to thank my committee members, Professor Farzin Zareian and Professor Mohammad Javad Abdolhosseini Qomi, whose work demonstrated to me and concern the support in Structural Engineering and Technology. Their work in this field was always transcend academia and provide a quest for our times.

This study was part of a funded project by SCHNELL™ HOME S.R.L., Fano, Italy. The technical input of Mrs. Lucia Manna and Mr. Pierluigi Pettinari Luigi is highly acknowledged.

In addition, a thank you my fellow Ph.D. Researchers, Mr. Islam Mohammed Rabie Farrag and Mr. Ehsan Mirnetaghi , Graduate Researchers, Mr. Swaroop S. Doddawadamth, Mr. Rahil Shrivastava and Miss Surbhi Dadlani, who helped me in experimental work, and whose enthusiasm for the work keeps the spirit high.

Last but not the least, I thank my fellow undergraduate researcher, Mr. Khalid Bafakih and Mr. Sina Sagha for participating on experimental part of the study.

ABSTRACT OF THE THESIS

Flexural Behavior of Two-Way Sandwich Slabs

By

Jivan Vilas Pachpande

Master of Science in Civil Engineering

University of California, Irvine, 2015

Professor Ayman S. Mosallam, Chair

This dissertation presents the details of the findings of a study focused on evaluating the structural behavior of three-dimensional (3D) cementitious sandwich panels with Expanded Polystyrene (EPS) foam core for two-way slab applications. In this study, both theoretical and finite element numerical analysis procedures were adopted to predict the performance of such slabs under out-of-plane loading conditions. The results from theoretical and finite element analysis were verified by comparison with full-scale laboratory tests conducted at the Structural Engineering Test Hall (SETH). The sandwich panels evaluated in this study comprise of expanded polystyrene foam sandwiched between high-strength mortar faces reinforced with cold-rolled steel wires in two directions. Two analytical methods were utilized in characterizing the flexural behavior of the sandwich slabs; mainly (i) Yield Line Theory, and (ii)finite element modeling using MARC-MENTAT software. In the finite element (FE) model, the concrete facings of the panel modeled using quadrilateral plate elements, whereas steel wire mesh is represented by beam elements. The FE model was analyzed by nonlinear static analysis. Numerical FE results are compared with experimental data to validate the numerical approach used. Based on the results of this research, it was concluded

that a simple MARC finite element model can be used to analyze the flexural behavior of these sandwich panels for two-way slab applications. Analytical results using FEA show good correlation with the experimental results. Furthermore, recommendations for future research in this area are presented.

Chapter 1

INTRODUCTION

The main objective of this study is to analyze the composite behavior of Expanded Polystyrene Sandwich (EPS) panels under concentrated load in two-way action using Finite Element Analysis (FEA).

For many years, research is being conducted to develop more efficient building light-weight materials that reduce the dead weight of the structure without compromising the strength and stiffness properties. One example of these materials is the orthotropic three-dimensional (3D) reinforced sandwich panels system. These panels can be very helpful in providing high-performance structural materials with less amount of concrete or mortar, in addition to its superior thermal insulation and acoustic properties.

The aim of this study is to predicate and simulate the flexural (out-of-plane) behavior of this system when used as floor/roof members. In order to accomplish this objective, analytical and numerical methodologies ae implemented. The first part of this study focuses on utilizing the Yield-Line Theory to analyze the flexural behavior of the sandwich two-slabs while the second part of the study focuses on developing a finite element model (FEM) to predict both the linear and nonlinear behavior of such innovative building system. The analytical and numerical results are then compared to the full-scale experimental results that were conducted on three sandwich slab specimens.

1.1 CEMENTITIOUS COMPOSITE FLOOR PANELS WITH EPS FOAM CORE

The orthotropic sandwich panels used in this study consist of a fire-retardant Expanded PolyStyrene (EPS) core surrounded by two steel wires meshes at each side of the EPS core. The complete sandwich structural element is produced by spraying or applying high-strength mortar of concrete at both sides of each panel. In order to provide connectivity between the two reinforced face sheets (i.e. steel wires/cementitious mortar faces) through-the-thickness steel wires are provided. The presence of the EPS foam core serves important and purpose in eliminating the unnecessary concrete and thus reducing the dead weight of the structure. In this scenario, the concrete is spaced away from neutral axis using EP which increases the moment lever arm and thus increasing the efficiency of the system. The mild steel reinforcement forms the 3D space truss in the system which provides the purpose of transverse shear stress transfer through weak EP core. It also provides the tension reinforcing area in the concrete at tension side. In addition, the EPS core provides superior thermal and acoustic insulation to these panels as compared to solid concrete slabs.

1.2 MATERIALS DATA

The material used in this study is manufactured by Schnell Home S.R.L. of Fano, Italy. The following paragraph provides summary of the properties of this system that was used in the analytical and numerical analysis.

1. High-Strength Cementitious Mortar: The cementitious mortar used in this study has a 28-day compressive strength (f'_c) of 5,000 psi (*34.50 MPa*) (*confirming to ACI 318-14 and IBC 2012)* The average mortar compressive strength value was obtained from tests per ASTM C109/C109M–11, "Standard Test Method for Compressive Strength of Hydraulic Cement Mortars" (*confirming ASTM C1140/C1140M-11*) Standards. The thickness of mortar of the compression side of the slab was 2″ (*50 mm*) and 1.5" (*38 mm*) on the tension side of the tested panel.

2. Galvanized Reinforcing Steel Wires: The reinforcement used was in the form of 9-gauge galvanized cold-rolled steel wires (*confirming to ASTM A-82 and ASTM A-185*) made up of cold rolled steel. The longitudinal steel wires were spaced at 3.15" (*80 mm*) O.C. and transverse wires were spaced at an equal distance of 2.95" (*75mm*) O.C., thus creating mesh opening of size 3.15" x 2.95" O.C. (*80 mm* x *75 mm*). The minimum reinforcement ratio to the gross cementitious area for each specimen was 0.0026, which confirmed with ACI 318-14 section 8.6.1. Steel wires were used to form the meshed face sheets and horizontal reinforcement that connected the opposing face sheets into a rigid three dimensional structure. The minimum reinforcement ratio for the tested slab specimens was 0.0039 for the 1″(25.4mm) thick shell. In both cases, the paneled slab system sufficed the minimum reinforcement ratio as per ACI 318-14 confirming its use as structural slab.

3. Expanded Polystyrene (EPS) Foam Core: The fire-retardant Expanded PolyStyrene cores used for the two-way slabs evaluated in this study has an average density of 0.90 pcf (14.42 kg/m^3) which confirmed with the ASTM C578-07a standard. Slab specimens, designated herein as "A" and "C", have an 8.5" (216mm) thick foam core while Slab "B" has a 7.0" (177.80mm) thick foam core A clear gap of 0.60" (15.25mm) was maintained between the reinforcement mesh and external surface of the EPS foam core to embed the steel wire mesh in the mortar during the construction of the finished Schnell slab panels. The EPS foam core had uniform undulations on the surface as shown in Figure (1-1).

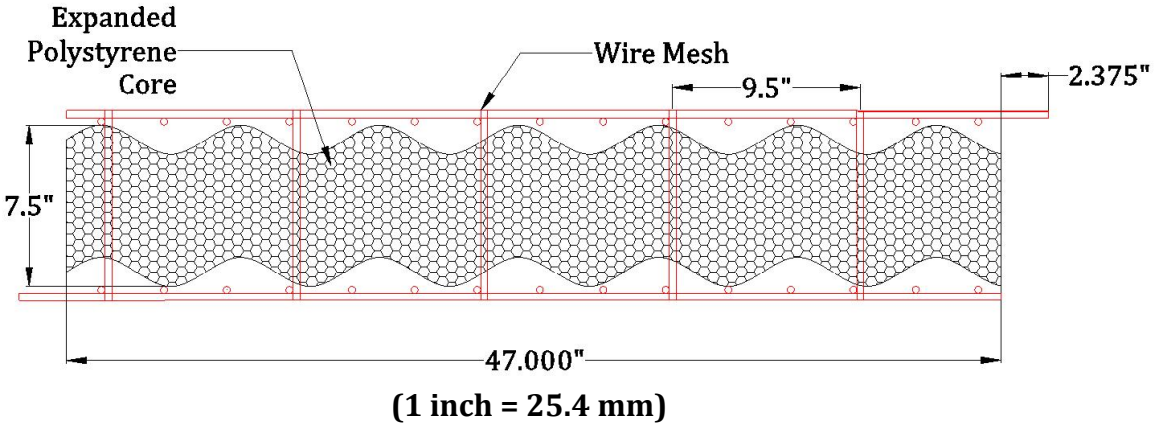

Figure (1.1): Expanded Polystyrene Core for 10.5" thick Slab

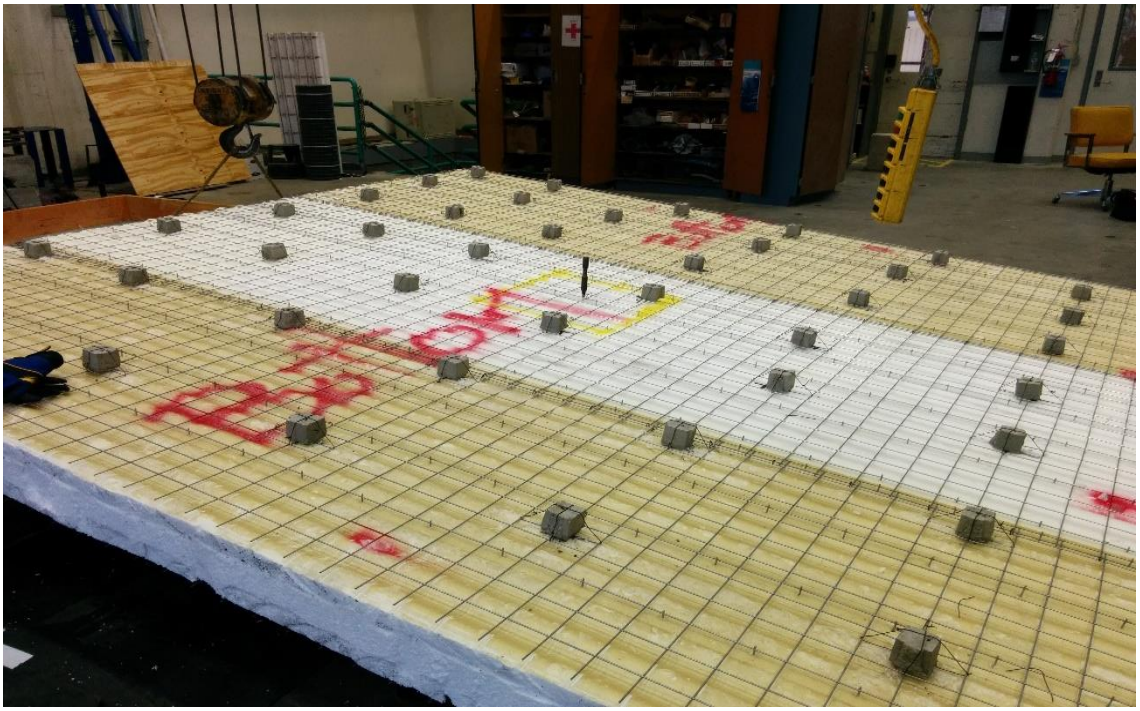

Figure (1.2): Expanded Polystyrene Foam Core used in Slabs

1.3 REINFORCEMENT SCHEDULE

As described earlier, the face steel meshes have a 3.15" (*80 mm*) X 2.95" (*75 mm*) mesh opening providing reinforcement in both longitudinal and transverse directions of each panel. Each sandwich panel has an overall dimension of 196" (*4980 mm*) X47" (*1195 mm*) and with different core thicknesses. The steel wire reinforcement along the longitudinal direction is spaced at 3.15" (*80 mm*) center-to-center while the wires along short side are spaced at 2.95" (*75 mm*) center-to-center. Furthermore, the wire mesh has extension of 2.375" (*60 mm*) along the short side on each face and on either side. This extension is provided to satisfy the transfer of forces along the edge of the panel and maintain continuity between two different panels. This can be seen in the Figure (1.1).

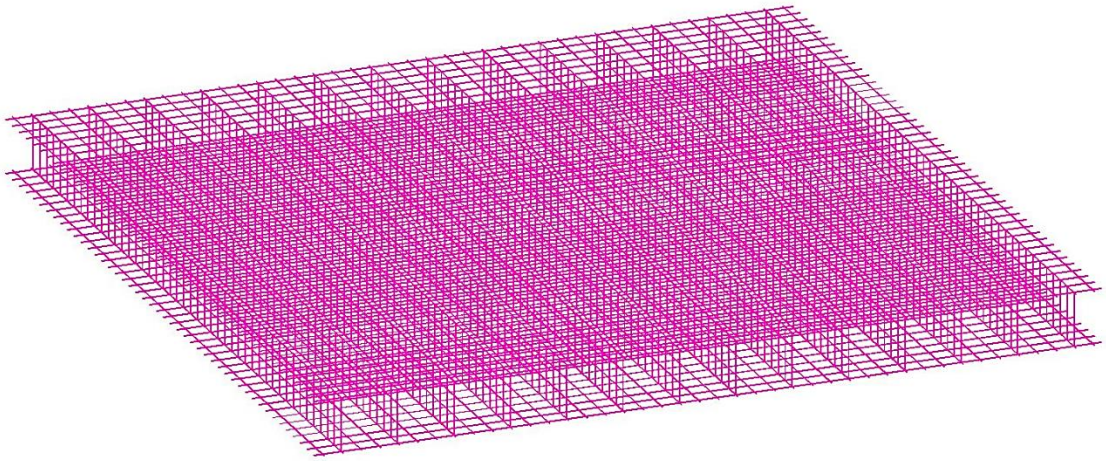

Figure (1.3): Reinforcement Mesh for Composite Slab

In addition to the flat steel meshes, parallel vertical through-the-thickness wires, connecting the two wire meshes, are inserted to provide an effective mean for partial composite action. These steel wires are space at 2.95" (*75 mm*) O.C. along the longitudinal direction of single panel and at 9.5" (*241 mm*) O.C. along the transverse direction of panel. These wires are designed to carry the entire transverse shear stresses, and therefore connect the top and bottom concrete reinforced cementitious faces. Hence, the transverse shear connectors play an important role in flexural behavior of sandwich slab. Details on the behavior of these slabs are discussed in the later chapters with numerical calculations.

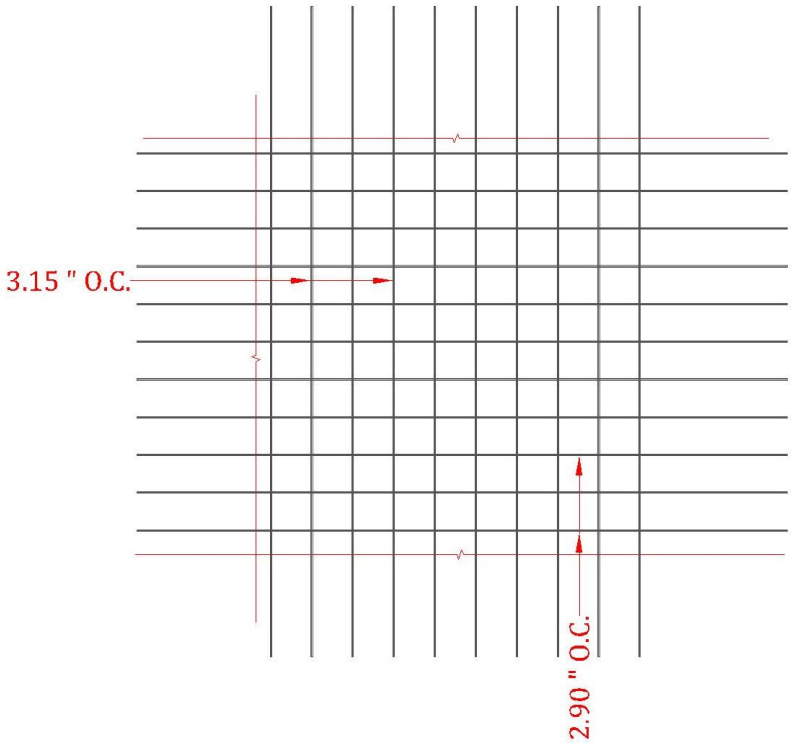

(1 inch = 25.4 mm)

Figure (1.4): Typical Spacing of Reinforcement

1.4 MOTIVATION AND PURPOSE OF STUDY

The light-weight orthotropic sandwich panels building system has been introduced to the construction industry few decades ago. Several forms of these panels are being produced; however, all systems have similar construction details. In designing these panels for out-of-plane applications such as floor and roof slabs, designers consider that these panes transfer the load in only one direction parallel to the longitudinal wire reinforcement. For this reason, all the construction completed to this date considers these roof/floor panels as one-

slab system by ignoring the contribution of the transvers reinforcement is ignored. This study is considered to be one of the first attempts to verify the ability of this system to form a floor/roof slabs capable of transferring the loads in two directions, and hence it could be designed as a two-slab system. The benefit of designing these panels as a 2-way slab system will provide additional economic advantage to these systems. In verifying such claim, both experimental and analytical procedures are needed. This is the main motivation behind this study that focuses on assessing the out-of-plane (flexural) behavior of two-slabs made of orthotropic sandwich panels described earlier. The analysis involved the use of the Yield Line Theory as well as non-linear finite element modeling simulating the flexural behavior of such light-weight orthotropic sandwich slabs.

The outcome of this research will allow engineers to analyze and design the composite floor panels with the correct assumptions associated with the cross section strain variation. Also, the analytical approach will help in developing the strain variation for the composite cross section and will enable in estimating the flexural properties of the cross section.

1.5 DESCRIPTION OF EXPERIMET PROGRAM

1.5.1 TEST PROTOCOL

The same test program was used to evaluate the three specimens subjected to out-of-plane concentrated loading at center. A loading protocol of 3 psi/s (*0.02 MPa/s*) was used for all specimens until failure occurred. Figure (1.5) shows the test configurations for the flexural evaluation of each specimen of composite slabs under

central distributed load. Figure (1.6) presents locations of string potentiometer (referred to hereafter as “String Pots”) that were used for the experimental program that is described elsewhere [1].

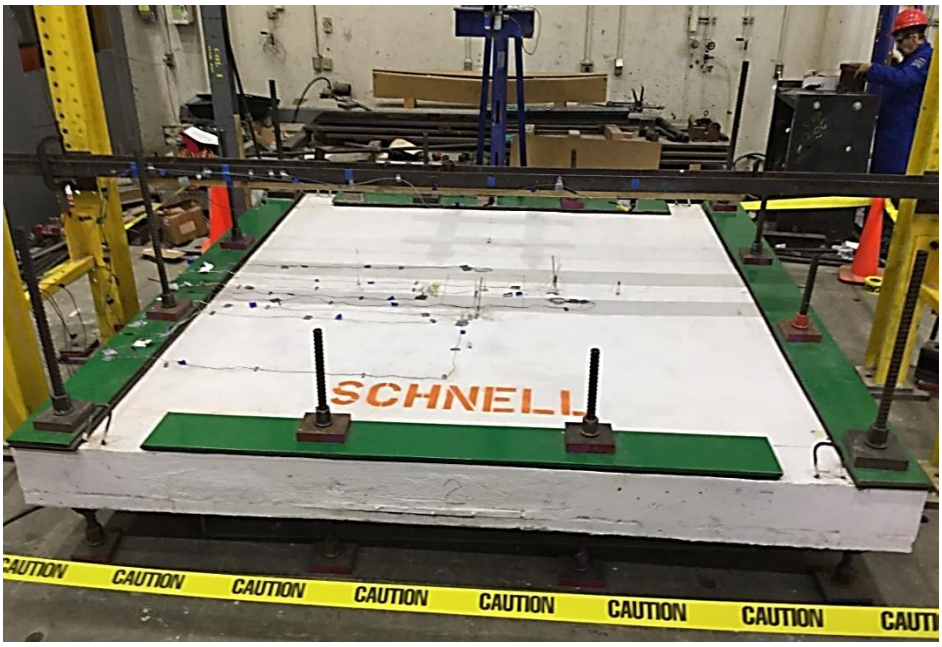

(a) Slab Specimen “A” Test Setup

(b) Slab Specimen “B” Test Setup

(c) Slab Specimen "C" Test Setup

Figure (1.5): Experimental Test Setup Configurations for Slab Specimens

1.5.2 DEFLECTION AND STRAIN MEASUREMENTS

To measure the deflection of specimens due to the point load application of hydraulic actuators, the built-in displacement transducer and several external noise, individually calibrated String Potentiometers (*String Pot*) were used. Figure (1.6) presents the location the string pots, strain gages placed on the mortar surfaces, and strain gages placed on steel wires. Figure (1.6 (b) and (c)) shows the locations of strain gages on the slab specimens. Electronic foil resistance strain gages (with 120 Ω resistance) were bonded to both mortar and steel wires surfaces at critical locations of all the slab specimens. All deflection, applied load and strain data was collected using a computerized National Instruments, data acquisition system. From the

recorded data, the Load vs. Deflection (P-Δ) curves and the stress/strain (σ/ε) curves were developed for each specimen.

The equipment used to complete the test program consisted of hydraulic pumps to generate force, hydraulic jacks to impart loads, high strength rods to assist in applying the load, pivots, test frames to transfer loads, tie-rods to constrain motion, strain gages and transducer to capture behavior, and data acquisition systems to record behavior.

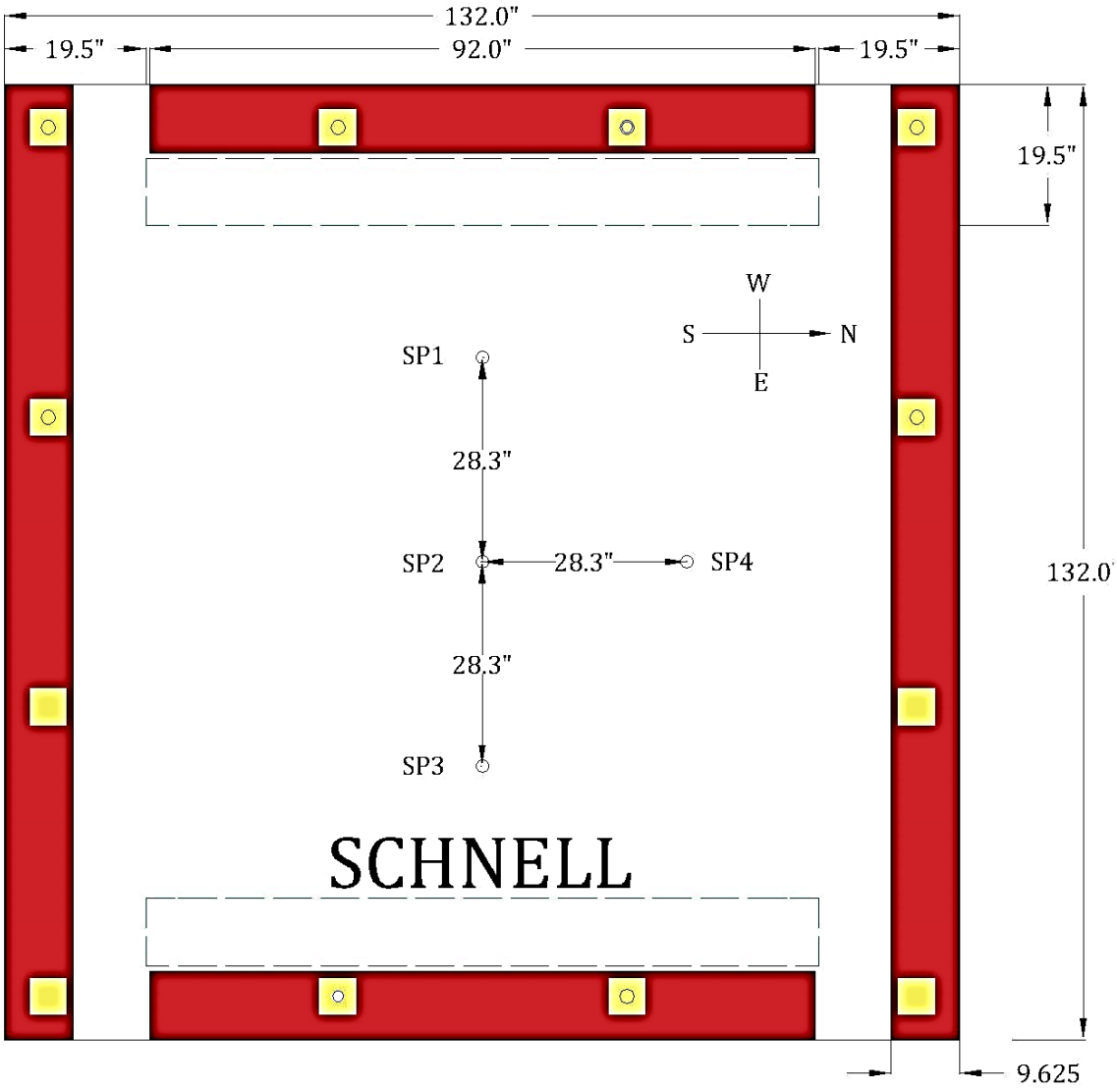

All Dimensions are in Inches (1 inch = 25.4 mm)

(a) Locations of String Pots

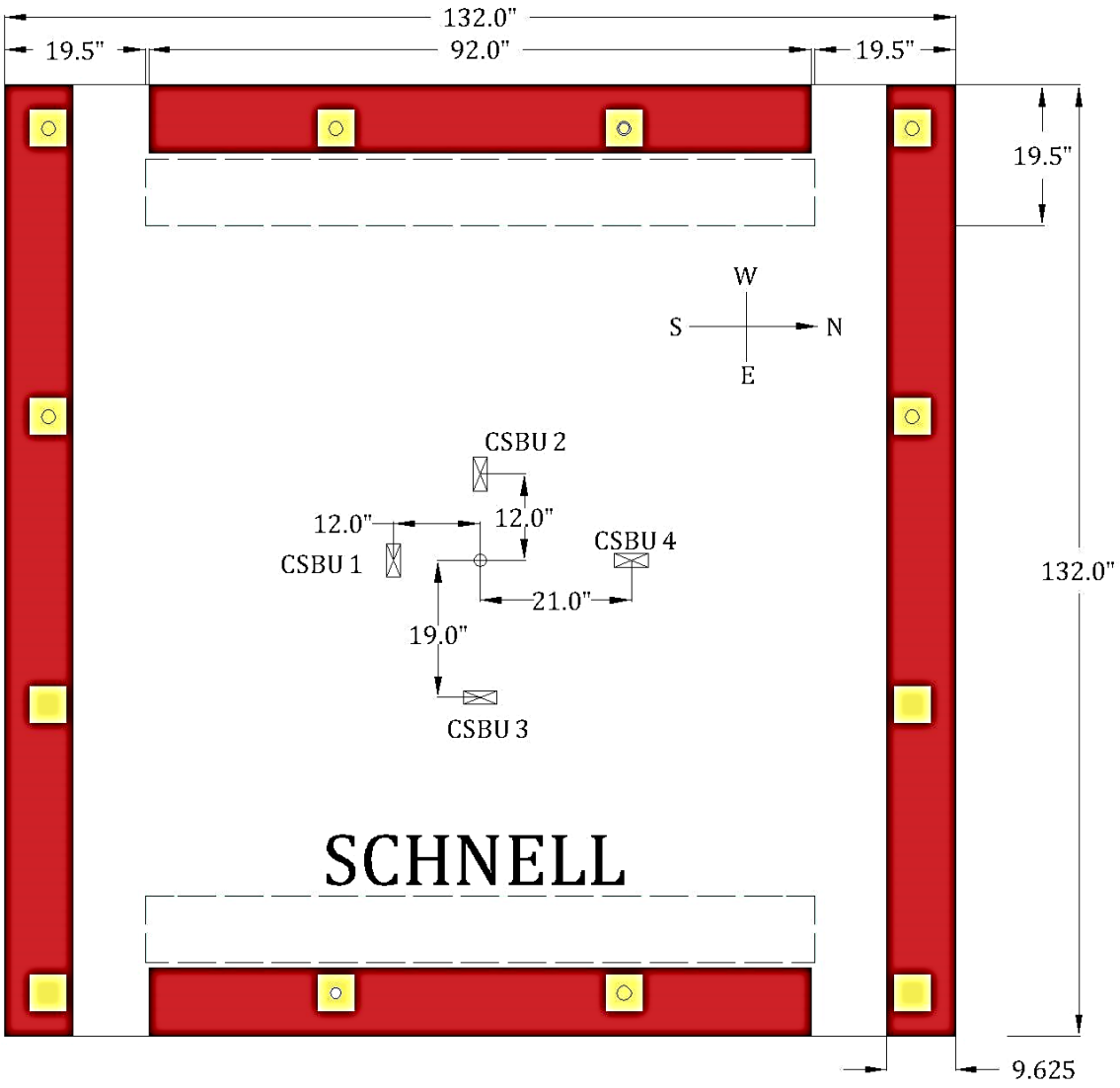

All Dimensions are in Inches (1 inch = 25.4 mm)

(b) Locations of Mortar Strain Gauges

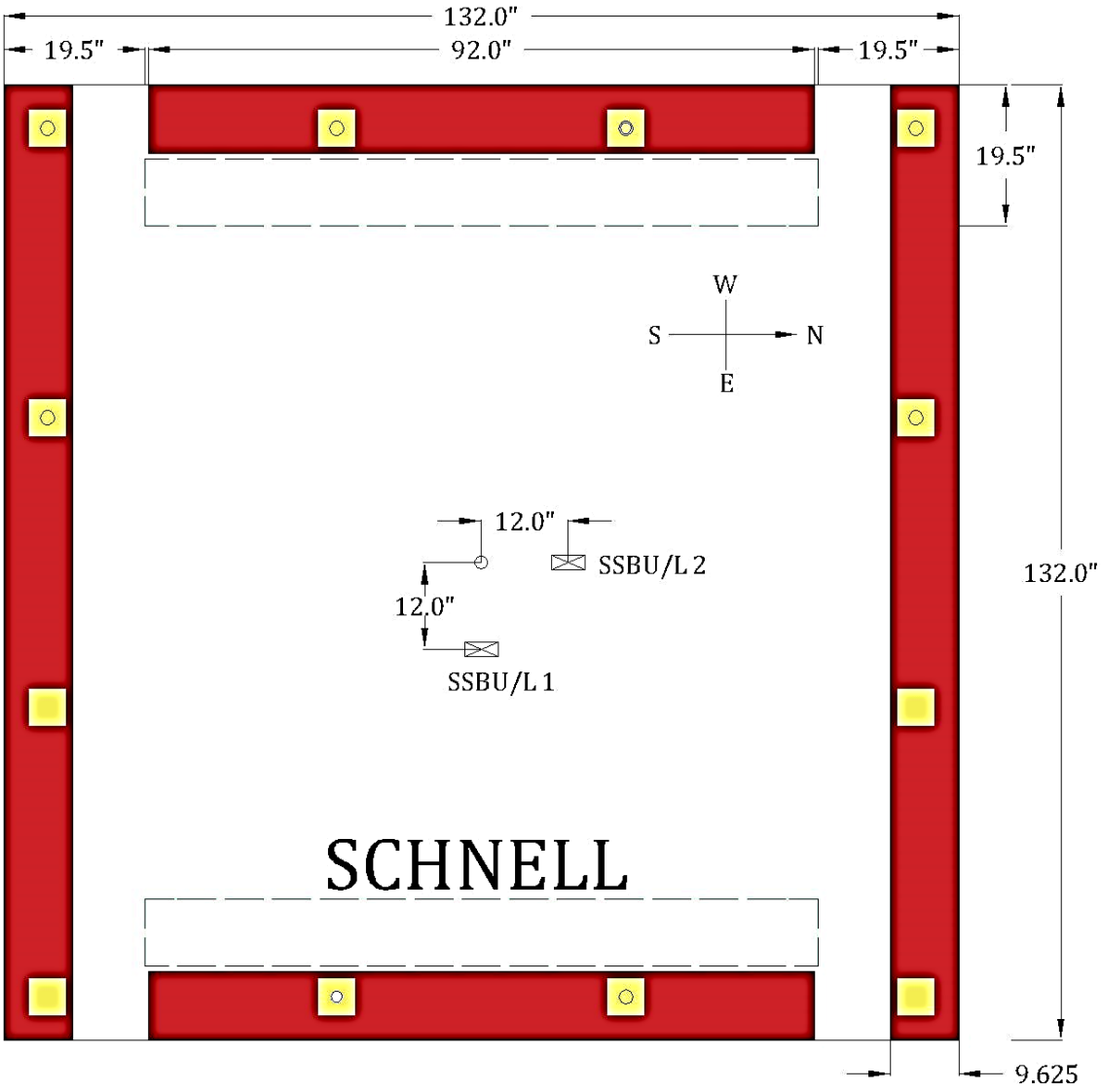

All Dimensions are in Inches (1 inch = 25.4 mm)

(c) Locations of Steel Strain Gauge

Figure (1.6): Locations of: (a) String Pots, (b) Strain Gages n Mortar Surface, and (c) Strain Gages on Steel Wires

1.5.3 BOUNDAY CONDITIONS AND SUPPORT SYSTEM

All of three sandwich slabs tested for verifying the analytical procedures were supported on four 12" (*305 mm*) deep wide-flange steel beams before the actual start of loading for supporting the dead-weight of the slabs. The fixed boundaries were created using ¾" (*19 mm*) thick steel plates of A36 grades. The steel plates were fixed to the slabs with high-strength rods. For Slab "A" and "B", twelve 1.5" (*38 mm*) diameter high-strength DYWIDAG THREADBAR® steel rods were installed and securely fastened to the slab. For Slab "C", the number of the DYWIDAG THREADBAR® steel rods were sixteen with a diameter of 1.0″ (25.40 mm) that were used to fix the steel plates with sandwich slabs.

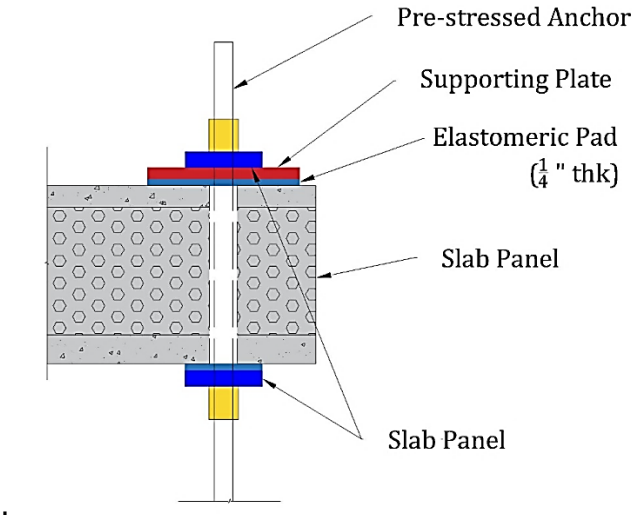

(1 inch = 25.4 mm)

Figure (1.7): Support System for Slab

In Figure (1.5), the supporting steel plates are shown in red color whereas; yellow color indicates the high strength rods. The high strength rods were fixed rigidly with the ground below using pre-stressing technique. The rods were tensioned to stress of 4,500 psi (*31.03 MPa*) so that the rods are completely fixed with slab and the possibility of displacement of supports during the loading process. Details of the test setup is reported by (Dadlani 2015).

Chapter 2

STRUCTURAL BEHAVIOR OF TWO-WAY SLABS

The reinforced concrete is the most widely used construction material nowadays in the construction industry. Almost all of the structural slabs utilizes reinforced concrete for resisting the floor loads. The floor slabs are classified as one way slabs and two way slabs. The two way slabs can resist loads for longer spans than the one way slabs and they are also efficient as well as economical. This chapter discusses about the behavior of two way slabs and the application of finite element analysis for two-way slab analysis.

Two way slabs are the structural elements which supports the floor loads by transferring in both directions of slabs. Two-way slab is the most widely used type of structural system in the construction industry because it as a very efficient and economical system. This can be explained with the help of Figure (2.1). If the beams are incorporated within the depth of the slab itself, it can be seen that the slab carries load in two directions. The load at point A may be thought as being carried from point A to point B and point A to point C by one strip of the slab. Furthermore, it can be visualized that load is being carried from point B to points D and E and point C to points F and, by other slab strips as indicated in Figure (2.1). Because the slab has to transfer loads in two orthogonal directions, the system is called as two-way slab system [1].

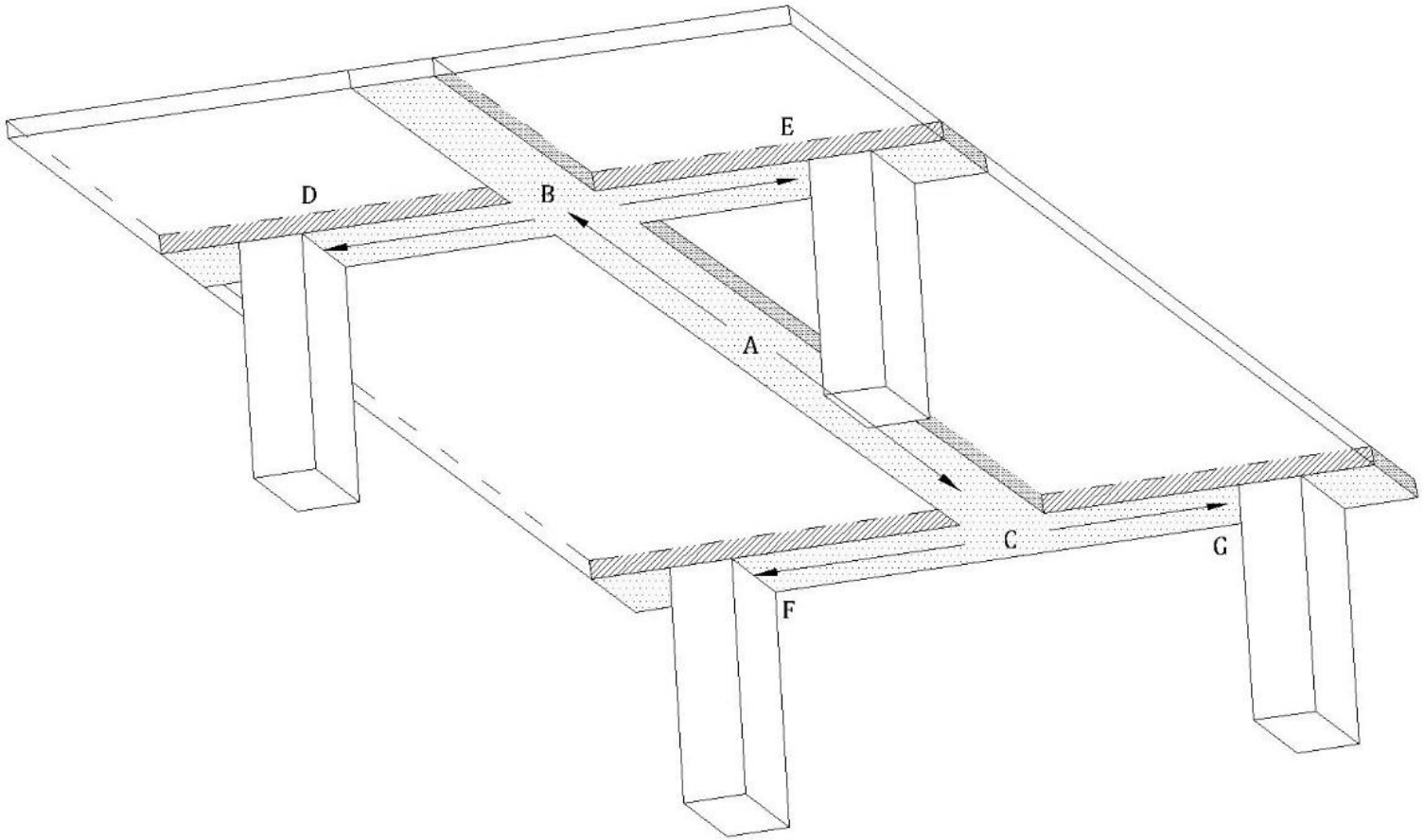

Figure (2.1): Load Path for Two-way Slab [MacGregor 2005]

2.1 TYPES OF TWO WAY SLABS

i) Flat Plate: These type of two slabs are usually used for lighter set of loads. This type is a slab of uniform thickness which is directly supported on the columns. Flat plates are considered economical as they can be constructed rapidly and they are most economical for spans from 15.0' to 20.0' (*4.5 m to 6 m*) [1]. This type of slabs is shown in Figure (2.2).

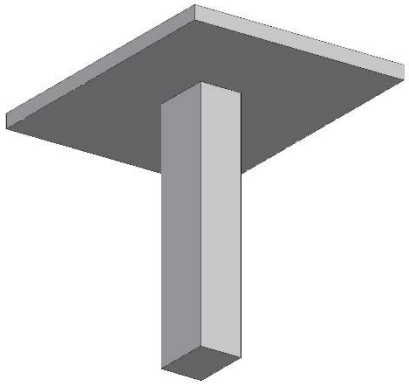

Figure (2.2): Flat Plates [Santos et.al. 2014]

ii) Flat Slab: For the larger spans and heavier loads, the flat slab systems can be used. The flab slab systems are very similar to the flat plate, but instead of directly supporting the slab on columns, the slab is thickened at the column locations with the help of drop panels as shown in Figure (2.3). When the span of the slabs is increased, the slab at the column locations has to transfer more vertical loads which requires more thickness of the slabs. This does not utilize the total thickness of the slab at the midspan, where bending moment has to be resisted. The drop panels increase the efficiency of the slab by increasing

the thickness at the column locations only. This slab system is very economical for supporting longer spans from 20.0' to 30.0' feet (*6.0 m to 9.0 m*) and heavier loads in excess of 100.0 psf (*4.8 kN/m²*) [1].

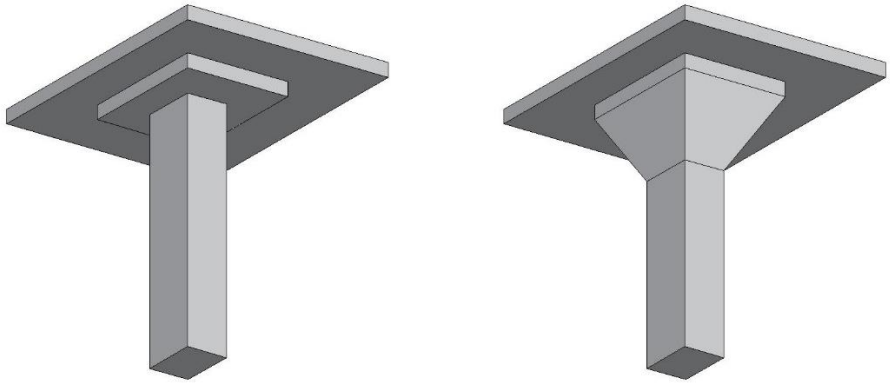

Figure (2.3): Flat Slabs with Drop Panels and Drop Caps [Santos et.al. 2014]

iii) Waffle Slab: For the larger spans in flat plates, the thickness of slab has to be increased and hence, the dead weight of the slab is increased. Hence, to reduce the weight of the slab and slab moments, the thick slab at midspan can be replaced by intersecting ribs in both directions which helps in saving the material. This type of system is called as a waffle slab or a two-way joist system [1] and it shown in Figure (2.4). Waffle slabs can be used effectively for spans up to 20.0' to 30.0' feet (*6.0 m to 9.0 m*) which support heavy loads also and it is commonly used in residential as well as office buildings [2].

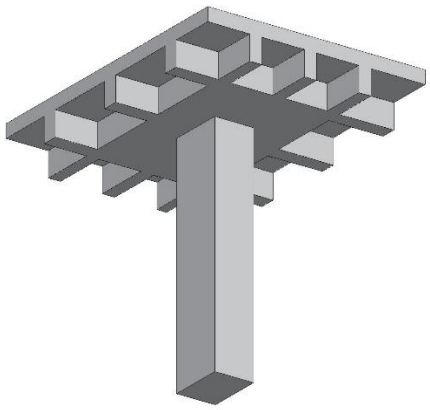

Figure (2.4): Waffle Slabs [Santos et.al. 2014]

iv) Two-way Slabs Supported with Beams**:** This type is the simplest type of slab in which the slab system is incorporated between some or all of the columns and the resulting slab panels have length to breadth ratio less than 2. This type is shown in the Figure (2.5).

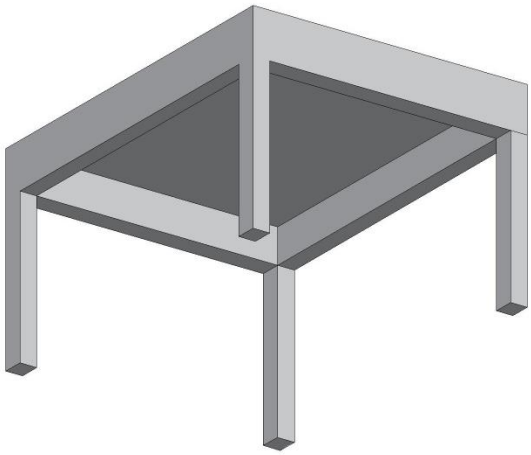

Figure (2.5): Two-way Slab supported by Beams [Santos et.al. 2014]

2.2 BEHAVIOR OF TWO-WAY SLABS

The behavior of two-way slab is very similar to the elastic thin plates before the cracking of the concrete occurs. Before the cracking of concrete occurs, the slab acts as an elastic plate till the cracking point, the deformation, stresses and strains can be calculated using an elastic analysis [2]. Once cracking occurs, the concrete in slab is no longer to carry the tensile stresses and this stress is transferred to steel embedded in concrete through bond stress. The stiffness of cracked region of the slab is no longer constant over the spread of the slab and hence the slab is no longer isotropic in nature. Even though it violates the assumptions in the elastic theory, the moments predicted by elastic theory are quite accurate [2].

After this phase, the yielding of reinforcement starts to occur in the regions of high moments and the yielding spread through the slab as moment gets redistributed from yielded region to non-yielded regions. If the slab edges are fixed, the yielding starts at the negative moment regions and it progresses along the edges forming the plastic hinges. These hinges spread along the edges of the slab as shown in Figure (2-6a) and eventually the new plastic hinges are formed along the edges as shown in Figure (2-6b). The plastic hinges are formed at mid-span as the positive moment at the mid-span of the slab increases due to moment redistribution caused by the negative plastic hinges.

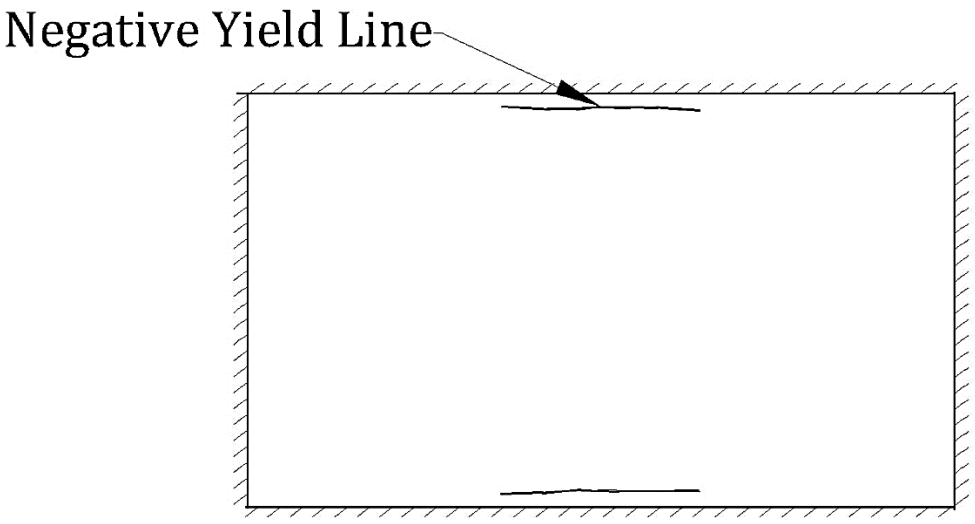

(a) Negative Yield Line Formation

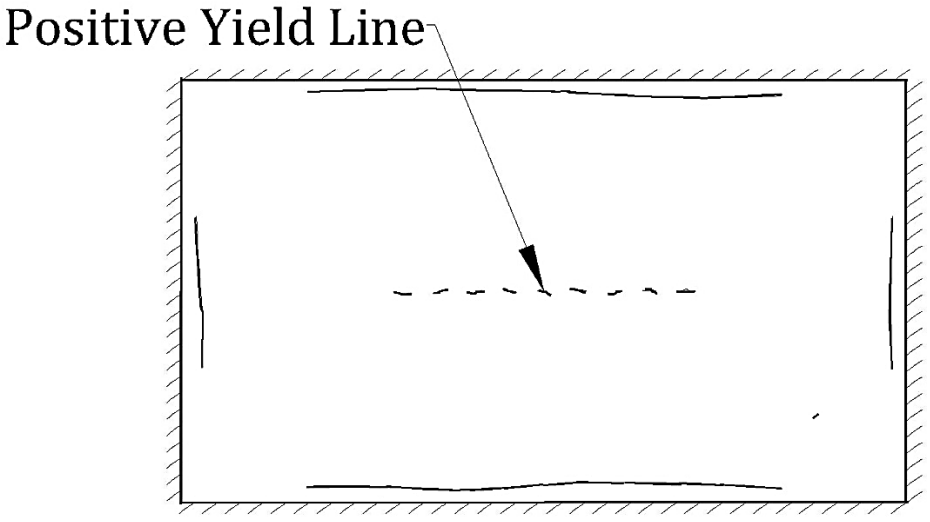

(b) Positive Yield Line Formation

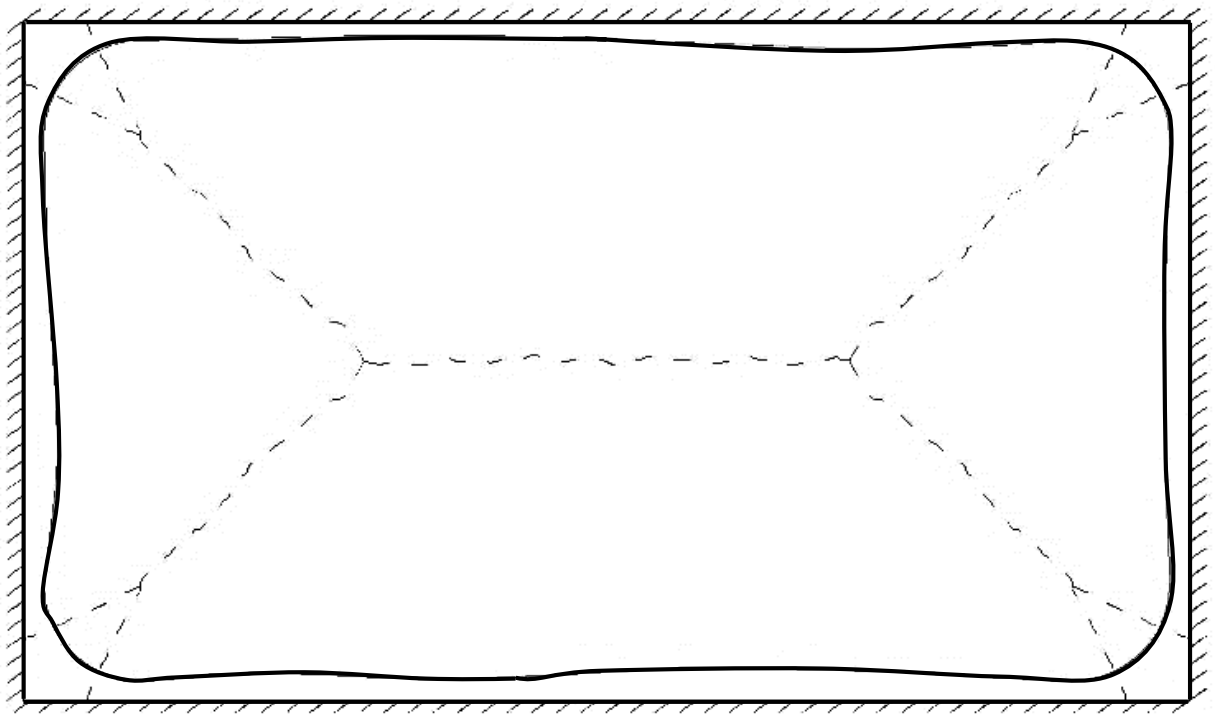

(c) Complete Yield Line Pattern for Two-way slab

Figure 2.6: Inelastic Action in Slab Fixed on Four Sides

As the load imposed on slab increases, the positive plastic hinges spread through the slab, which are called as the yield lines, and they divide the slab into triangular and trapezoidal plates as shown in Figure (2-6c). This analysis is numerically explained in the next chapter under yield line analysis. After the yield lines are completely spread over the slab, the plastic hinge mechanism is formed, and the failure of the slab occurs.

2.3 ANALYSIS METHODS FOR TWO-WAY SLAB

The analysis of a two-way slab is complicated because of the load distribution in both directions of slab. There are four major methods for analyzing and designing the two way slabs, which are popularly used nowadays and these methods are stated as follows:

i) Direct design method: This method is very popular analytical and design method and is widely used in practice. The slab plate is divided into a series of column- and middle-strips. The moment for the entire slab plate is determined using the load and the clear span, which is called *slab static moment* (M_0). The slab static moment is then multiplied by different coefficients that are defined in building codes to find the maximum moments in strips [4,5]. In the direct design method, the moment curves in the direction of span length need not to be calculated using the sophisticated elastic analysis. Figure (2.7) shows the longitudinal moment diagram for the typical interior span of the equivalent rigid frame in a two-way floor system [4]. ACI 318-14 § 8.10.4 provides the coefficients for distributing this moment transversely to the slab over the span Ln as shown in Figure (2.7). The positive moment at mid-span for the interior span is given as 0.35M0 and the

negative moment is 0.65M0. These coefficients change as the condition of slab changes. ACI 318-14 § 8.10.4 provides the coefficients for the slab under five different conditions of the exterior depending upon the edge conditions.

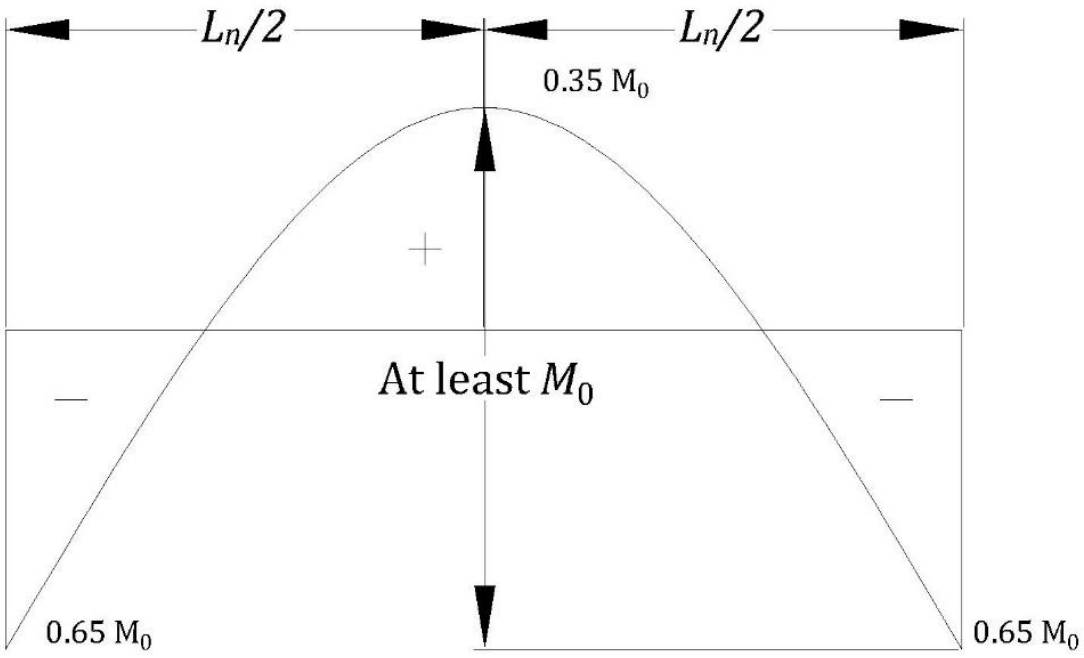

Figure (2.7): Interior Span Moment Diagram for longitudinal span

ii) Yield Line Theory: The design methodologies mentioned in ACI 318-14 are based on the elastic analysis of the structure as a whole. In the indeterminate structure, once the moment strength at one or more points is reached, discontinuities are developed in the elastic curve at those points and hence the elastic analysis is no

longer valid. Because of the redistribution of moments which happen in the two way slabs as explained earlier, the sections of the discontinuities are form a mechanism in structure at which the structure collapse. The location in the slab where discontinuities occur, are called "*plastic hinges*" and these plastic hinges divide slab into series of triangular and rectangular plates [4]. The regions or sections where plasticity (yielding) occur are called as "yield lines" and these lines are shown in Figure (2.6).

The yield line analysis uses *rigid plastic theory* to evaluate the failure loads corresponding to given plastic moment resistance of the yielded sections. It is very economical and versatile method for analysis of two way slabs and estimating the ultimate load carrying capacity, however, this method does not provide any idea about the deflection of the slab at failure and the load at which the first yielding occurs in slab. Ingerslev [6] first did yield line analysis for simply supported slabs using the normal moment method which assumes the equilibrium between loads and only bending moments acting at yield lines. Johansen [7,8] refined the yield line analysis by applying the virtual work method to the yield mechanisms of certain yield patterns and discovered that the results were different from Ingerslev's normal moment method because of shear and twisting moments acting at yield lines. The basic principle of yield line analysis is that the yield lines must divide the slab into different parts in so as to form the failure mechanism [9].

Johansen restricted this basic principle to the straight lines that divide the slab into plane regions. However, as it can be seen in real load tests, real yield lines, and consequently regions bounded by them, are very frequently curved. This curvature can be produced by elastic deformations or by partial cracks, very visible in real tests [9]. The existence of curved yield lines for certain boundaries is very important for this work because, as we shall see later, in those cases ''correct'' and real yield lines must be necessarily curved. All this was confirmed using simulated annealing method by Vázquez [10]. It can be inferred that yield line shall follow a certain set of rules to validate the failure mechanism of the slab. The location and orientation of the yield lines are quite evident in case of simple slab as shown in Figure (2.6). For other slabs it is advisable to use the different set of rules for determining the yield line pattern. When the slab is in verge of collapse, because of real plastic hinges to form mechanism, axes of rotation are located along the lines of support or over the point of column locations and the slab segments rotate about the axes of rotations. Because the yield line contains all points common to these two planes, it must contain the point of intersection of two axes of rotation, which is also common to the two planes. Hence the yield line (or *extended yield line*) must pass through the point of intersection of the axes of rotation of the two adjacent slab segments to from mechanism.

iii) Equivalent Frame Method: Equivalent frame method is an analysis tool which models a two-way slab as one-way frame. It has been used as ACI's standard method for analysis of two-way slab including post-tensioned slab since 1970. The word *equivalent frame* dignifies that this analysis frame is different from usual

rigid frame model where slab or beams are connected to columns as rigid connection. In equivalent frame, beam is connected to column via torsional member. The rotation at the end of beam is no longer equal to that of column as in rigid frame case.

The slab is divided into a series of equivalent frames running in the two directions of the building. These frames consist of the slab, any beams if exists, and the columns on above and below levels. For gravity load analysis, the ACI 318-14 code allows analysis of an entire equivalent frame extending over the height of building, or each floor can be considered separately, with the far ends of the columns fixed. These frame then are divided into column and middle strips. The column stiffness is calculated by using inverse flexibility matrix or by static consideration of global stiffness matrix. The columns and slabs are assembled as equivalent frames as shown in Figure (2.8).

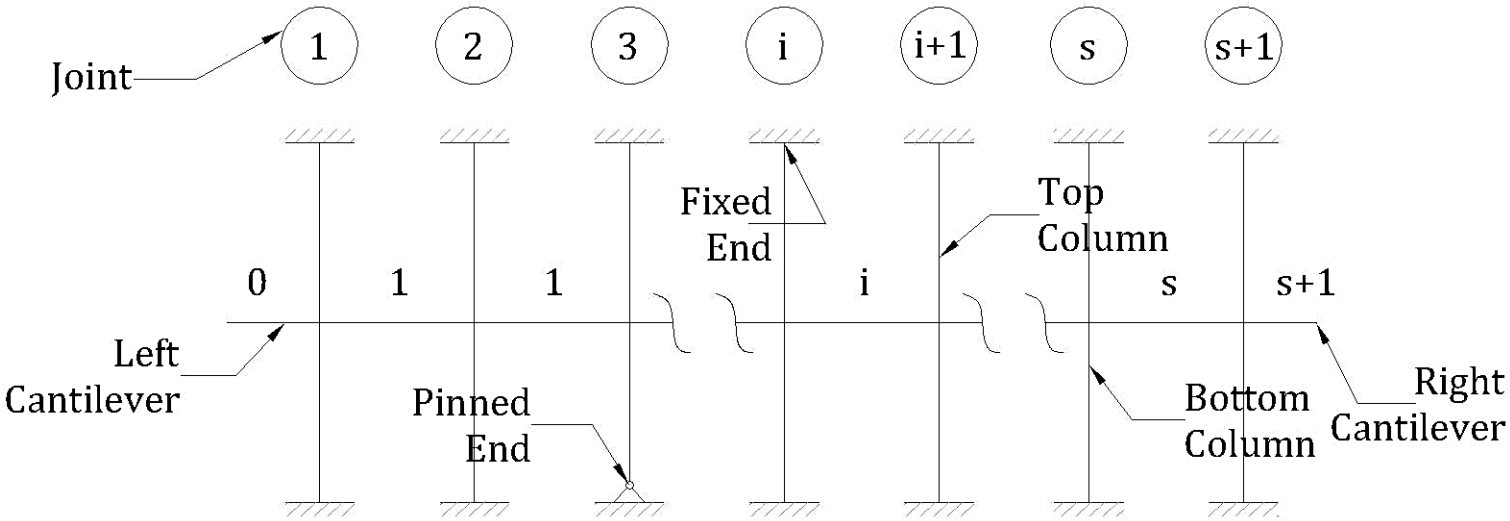

Figure (2.8): Equivalent Frame for Two-way Slab

iv) Strip Design Method: This method was developed by Hillerborg [11] and it is based on the lower bound theorem of the theory of plasticity, which means in in principle leads to adequate safety for the limit states, provided for that the reinforced concrete slab has a sufficiently plastic behavior. The lower bound theorem is usually formulated to check the load bearing capacity of a given structure. In the strip method, an approach has been chosen which instead aims to design the reinforcement so as to fulfil the requirements of the theorem. The complete equilibrium considered in this method contains bending moment in two directions of the slab and torsional moments with regard to these directions. However, consideration of torsional moments complicates the analysis and design procedure and it yields more reinforcement, hence, analysis and design without torsional moments is preferred wherever its possible.

The simple strip method the load is assumed to be carried by strips that run in the reinforcement direction and no torsional moments act in these strips. This method can only be applied where the strips are supported in such a way that they can be treated like beams. It cannot be applied for the strips supported by column and special advanced technique are required for determining the solution which is also known as advanced strip design method. This method is very powerful and simple for many practical applications, however, it cannot be easily applied for the irregular slab layouts and loading conditions [11].

An alternative technique of treating the slab with column supports or other concentrated supports is by means of the simple strip method combined with support bands. This method is most general and it can be applied in all slab layout and loading conditions. It shall be used when the requirement for other two methods are not met, but it requires more time consuming analysis as compared to the other two methods.

2.4 REVIEW OF ELASTIC PLATE BENDING THEORY

Slabs can be treated as thin elastic plates where bending occurs in both directions when subjected to out-of-plane loads. In case of the pure bending of prismatic bars, the rigorous solution for the stress distribution is obtained by assuming that the cross sections of bar remain plane during bending and rotate only with respect to their neutral axes so that the cross section is always normal to the deflection curve. The plates are subjected to combination of such bending action in two directions [12]. All of sandwich slabs tested in this program have a width-to-thickness (b/h) ratio greater than 5, therefore they can be distinguished as *thin elastic plates*.

2.4.1 ASSUMPTIONS FOR ELASTIC PLATE BENDING ANALYSIS

(i) The plate material is linearly elastic and follows Hooke's law,

(ii) The plate material is homogeneous and isotropic. The elastic deformations are characterized by Young's modulus E and Poisson's ratio (ν),

(iii) The thickness of the plate is small as compared to its lateral dimensions. The normal stress in the transverse direction can be neglected compared to the normal stresses in plane of the plate,

(iv) The cross section follows Bernoulli's bending theory meaning that the points on a straight line normal to neutral plane (plane of zero strain) remain in straight line after bending also,

(v) The deflection (w) of the plate is small as compared to the thickness of the plate. The curvature of the plate after deformation can be derived from second order differentiation of deflection (w),

(vi) The center plane of the plate is assumed to be stress free, and

(vii) Loads are applied in the normal direction of the center plane.

2.4.2 DIFFERENTIAL EQUATION FOR ELASTIC PLATE BENDING

Consider the rectangular plate shown in Figure (2.9) and assume that it is subjected to the bending moments per unit length of the edges parallel to the x and y axes are M_x and M_y. The moments are considered as positive since they create compression above the neutral axis and tension below it. The strains in x and y directions at distance z from the neutral plane are given in the equation (2.1).

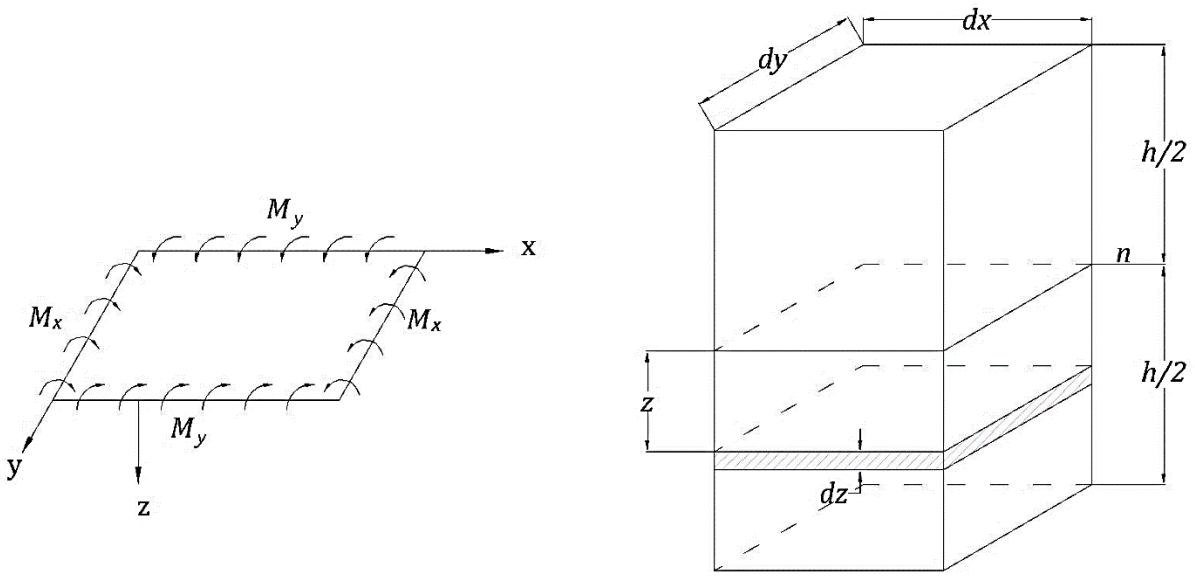

(a) Plate Subjected to Moment (b) Plate element

Figure (2.9): Pure Bending of Plate Element

$$\varepsilon_x = \frac{z}{\rho_x} \quad ; \quad \varepsilon_y = \frac{z}{\rho_y} \tag{2.1}$$

where, ε_x and ε_y are the strains and $1/\rho_x$ and $1/\rho_y$ are the curvatures in *x* and *y* directions respectively. From Hooke's law, it can be derived that

$$\varepsilon_x = \frac{1}{E}(\sigma_x - \nu\sigma_y) \quad ; \quad \varepsilon_y = \frac{1}{E}(\sigma_y - \nu\sigma_x) \tag{2.2}$$

where, σ_x and σ_y are stresses in *x* and *y* directions respectively. From the stress-strain relationship, normal stresses are derived from equations (2.1) and (2.2) as per following equations,

$$\sigma_x = \frac{Ez}{1-\nu^2}\left(\frac{1}{\rho_x} + \nu\frac{1}{\rho_y}\right) \quad ; \quad \sigma_x = \frac{Ez}{1-\nu^2}\left(\frac{1}{\rho_y} + \nu\frac{1}{\rho_x}\right) \tag{2.3}$$

The normal stresses can be converted to resisting couples which must be equal to external moments. The relationship between normal stresses and external moments is given in form (2.4),

$$\int_{-h/2}^{h/2} \sigma_x z dy dz = M_x dy \ ; \int_{-h/2}^{h/2} \sigma_y z dx dz = M_y dx \tag{2.4}$$

From the equations (2.3) and (2.4), it can be derived that

$$M_x = D\left(\frac{1}{\rho_x} + \nu \frac{1}{\rho_y}\right);\ M_y = D\left(\frac{1}{\rho_y} + \nu \frac{1}{\rho_x}\right) \tag{2.5}$$

where,

$$D = \frac{E}{1-v^2}\int_{-h/2}^{h/2} z^2 dz = \frac{Eh^3}{12(1-\nu^3)}$$ and h is the thickness of the plate

The quantity *D* is called as "*flexural rigidity of the plate"* [2,12]. Assumption iv is sufficiently accurate as long as the deflections are small in comparison with its thickness *h*. Some deformations in the middle surface will be produced if this assumption is violated and derivation of stress shall consider these deformations. The deflection *w* can be related with the curvature as shown in the equation (2.6)

$$\frac{1}{\rho_x} = -\frac{\partial^2 w}{\partial x^2}\ ;\ \frac{1}{\rho_y} = -\frac{\partial^2 w}{\partial y^2} \tag{2.6}$$

Therefore, the unit moments in acting along *x* and *y* directions is given by the equations as follows,

$$M_x = -D\left(\frac{\partial^2 w}{\partial x^2} + \nu \frac{\partial^2 w}{\partial y^2}\right);\ M_y = -D\left(\frac{\partial^2 w}{\partial y^2} + \nu \frac{\partial^2 w}{\partial x^2}\right) \tag{2.7}$$

Now, in considering the case of bending of plate by distributed load acting perpendicular to the middle plane of plate by distributed load of intensity q acting along z direction i.e. normal to the middle plane of the plate. It can be derived that the vertical shearing forces per unit length Q_x and Q_y because of the load q acting on the plate are given as in form (2.8),

$$Q_x = \int_{-h/2}^{h/2} \tau_{xz} dz \; ; \; Q_y = \int_{-h/2}^{h/2} \tau_{yz} dz \tag{2.8}$$

where, τ_{xz} and τ_{yz} are the vertical shearing stresses in x and y directions. The variation of , τ_{xz} and τ_{yz} along small distances can be neglected, and it is assumed that the resultant shearing forces $Q_z\,dy$ and $Q_y\,dx$ pass through the centroids of the sides of element. For the bending and twisting moments per unit length, it can be assumed that,

$$M_x = \int_{-h/2}^{h/2} \sigma_x z dz \; ; \; M_y = \int_{-h/2}^{h/2} \sigma_y z dz \tag{2.9}$$

$$M_{xy} = -\int_{-h/2}^{h/2} \tau_{xy} z dz \; ; \; M_{yz} = \int_{-h/2}^{h/2} \tau_{yx} z dz \tag{2.10}$$

In the equations of the vertical shear force, bending moments and twisting moments, it can be seen that all of them are functions of x and y. As we move to the other surface on right of element at distance dx, the corresponding quantities equal to as given in equation (2.11),

$$Q_x + \frac{\partial Q_x}{\partial x} dx \; ; \; M_x + \frac{\partial M_x}{\partial x} dx \; ; \; M_{xy} + \frac{\partial M_{xy}}{\partial x} dx \tag{2.11}$$

After consideration of the equilibrium of the element, it can be seen that all vertical forces parallel to the z-axis and that the couples are represented by vectors normal to the z-axis [12]. The equilibrium condition equation is given as form (2.12),

$$\frac{\partial Q_x}{\partial x} dxdy + \frac{\partial Q_y}{\partial y} dydx + qdxdy = 0 \tag{2.12}$$

or,

$$\frac{\partial Q_x}{\partial x} + \frac{\partial Q_y}{\partial y} + q = 0 \tag{2.13}$$

By taking moments of all forces about *x*-axis and considering the directions of the forces,

$$\frac{\partial M_{xy}}{\partial x} dxdy - \frac{\partial M_y}{\partial y} dydx + Q_y dxdy = 0 \tag{2.14}$$

Since the moment due to force Q_y and load q are neglected because of the small quantities of the higher order. Hence, after simplification it can be inferred that,

$$\frac{\partial M_{xy}}{\partial x} - \frac{\partial M_y}{\partial y} + Q_y = 0 \tag{2.15}$$

Similarly, for *y*-direction, if moments with respect to *y*-axis are taken, the moment equilibrium is given as,

$$\frac{\partial M_{yx}}{\partial y} + \frac{\partial M_x}{\partial x} - Q_x = 0 \tag{2.16}$$

Substituting values of Q_x and Q_y in form of M_x, M_y and M_{xy} and putting M_{yx}=-M_{xy} in the force equilibrium equation (2.14),

$$\frac{\partial^2 M_x}{\partial x^2} - 2\frac{\partial^2 M_{yx}}{\partial x \partial y} + \frac{\partial^2 M_y}{\partial y^2} = -q \tag{2.17}$$

This is the *finite element equation* for the elastic plate bending and this equation is widely used for two-way slab analysis. If the equation (2.17) for plate is further simplified in terms of the deflection *w* under influence of load *q,* the equation becomes as given in form (2.18)

$$\frac{\partial^4 w}{\partial x^4} + 2\frac{\partial^4 w}{\partial x^2 \partial y^2} + \frac{\partial^4 w}{\partial y^4} = \frac{q}{D} \tag{2.18}$$

The equations (2.17) and (2.18) are purely static equations and they can be applied in finite element analysis regardless of behavior of the plate material [2].

2.5 FINITE ELEMENT ANALYSIS FOR TWO-WAY SLABS

Finite element modelling of two-way slab helps in obtaining accurate and efficient numerical solutions [13]. In addition to the accuracy of the solutions, finite element method provides ability to determine the various failure modes and it also accounts for the material plasticity, cracking of concrete and also the large deformations of the slab [2]. Zienkiewicz [15] first introduced finite element analysis for the two-way slab systems where he applied the general finite element method to flat plates and presented the formulation of boundary conditions for these systems. The linear elastic analysis for applied to orthotropic slab systems and Zienkiewicz [15] demonstrated the ease with which the slab can be coupled with the frame members. The effect of torsional bending component in two-way slab was first introduced by Wood [16]. Wood and Armer [17] investigated the effect of twisting moments in the longitudinal moments as it greatly affected the capacity of the slab. A good agreement of the results from linear finite element analysis was obtained as that of the exact solutions.

However, the linear finite element analysis cannot be applied for the material when the behavior changes from elastic to plastic as the stress in element increases, i.e., Hooke's law is no longer valid in this region. Also, for reinforced concrete slabs, when the concrete cracks,

the section modulus of cracked section is different than that of the uncracked section. This effect can be considered in the linear finite element analysis. Hence, nonlinear method was introduced in analysis of concrete sections for accounting the modified stiffness. The first published works dealing with nonlinear finite element analysis of concrete systems emerged in the late 1960s [14]. These studies focused on various aspects of element formulation, including crack propagation and the bonding of reinforcement. Jofriet and McNiece [17] formulated slab analysis model based on effect of cracking and its orientation with respect to the slab's coordinate system, the rigidity of the cracked region and the rigidity of steel with relation to the crack propagation. A step based bilinear moment curvature relationship was introduced by Jofriet and McNiece [17] in the program to simulate progressive cracking. This approach is referred as "*modified stiffness model"* [14].

The nonlinear finite element analysis was applied to the slabs of arbitrary shape by Famiyesin and Hossain [18]. They applied a three-dimensional degenerated layered shell reinforced concrete model to determine model parameter values to calibrate the nonlinear analysis of fully restrained slabs, with the goal of extension to arbitrary configurations through parametric sensitivity studies. The resulting parameters were applied to thirty-six previously tested slabs, with the accuracy of strength determination within a mean value of 2% of experimental data. Even though the finite element analysis has numerous advantages over the conventional and approximate methods of analysis, this tool must be used carefully. The definitions like properties of materials, boundary conditions, element type, etc., shall be defined with care. Otherwise, this method can provide catastrophic results also, if modeling definitions are not assigned correctly.

Chapter 3

THEORETICAL ANALYSIS OF TWO-WAY EPS CONCRETE SLAB

The paneled slabs evaluated in this study are classified as sandwich plates. Sandwich composite panels has been used for decades by the aerospace industry. However, these aerospace type sandwich plates and commonly manufactures with aluminum alloy or polymer composite face sheet with different types of cores such as aluminum and composite honeycomb. This type of composite construction has superior flexural rigidity coupled with light-weight properties as compared to solid plates. The same principal was used in developing the 3D cementitious sandwich panels used in this study.

3.1 COMPOSITE BEHAVIOR OF 3D CEMENTITIOUS SANDWICHED PANEL

The sandwiched panel behavior can be explained with the help Figure (3.1). The concept behind the composite construction is similar to that of the steel wide flange beam profiles that were developed many decades ago by the steel industry. As shown in Figure (3.1), the high-strength/stiffness face sheets contribute to resist bending stresses while the core resists both vertical and transverse shear loads, and stabilizes the cross section from warping or buckling [19].

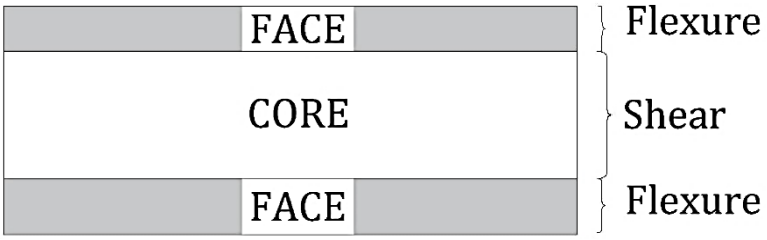

Figure (3.1): Composite Sandwich Construction

When the sandwiched composite member is subjected to flexure, the stiff enough core keeps the faces at proper distance to resist bending efficiently, and it also provides adequate horizontal shearing strength so that the faces do not slide off. If the core is not stiff enough to carry the horizontal shear effectively, then the faces won't act together and eventually the composite action would be lost. The core also prevents face under compression from local buckling failure and hence sandwiched construction proves to be strong and stiff enough and light weight at the same time [20]. In the sandwich slabs studied in this investigation, the structural mortar is place on the faces and core is made up of EPS fire retardant foam. The cold-rolled welded steel wire meshes are embedded in concrete at each face and they are connected with each other with vertical shear connectors. The through-the-thickness steel parallel shear connectors are introduced as the expanded polystyrene is very weak as compared to the concrete faces and it is not stiff enough to carry transverse shearing force.

3.2 CAPACITY PREDICTION FOR EPS CONCRETE PANEL

This section provides the estimation of the moment capacity of the sandwich slabs using modified ACI 318-14 code procedures. The capacity is used to predict the failure load for the two-way slab with the help yield lie theory and then compared with the experimental data. There are following important assumptions used in prediction the moment capacity of sandwich slabs.

i) The section follows full composite action meaning that the shear connectors have enough shear capacity to carry horizontal shear,

ii) The composite section remains plane even after bending i.e. it follows Bernoulli's bending theory,

iii) The strength of polystyrene is neglected and it is assumed that it does not contribute to the strength of cross section,

iv) The average thickness of concrete is considered over the polystyrene and change in thickness of concrete because of wavy structure of foam is neglected,

v) The contribution from compression steel is neglected i.e. singly reinforced action is assumed,

vi) The width of section assumed for analysis is 1 foot, hence b = 12", and

vii) The neutral axis lies at the contact location of concrete and expanded polystyrene.

Figure (3.2) shows the strain distribution in the cross section based on the assumption number ii [22]. It also shows the free body diagram for cross section of EPS concrete panel under bending.

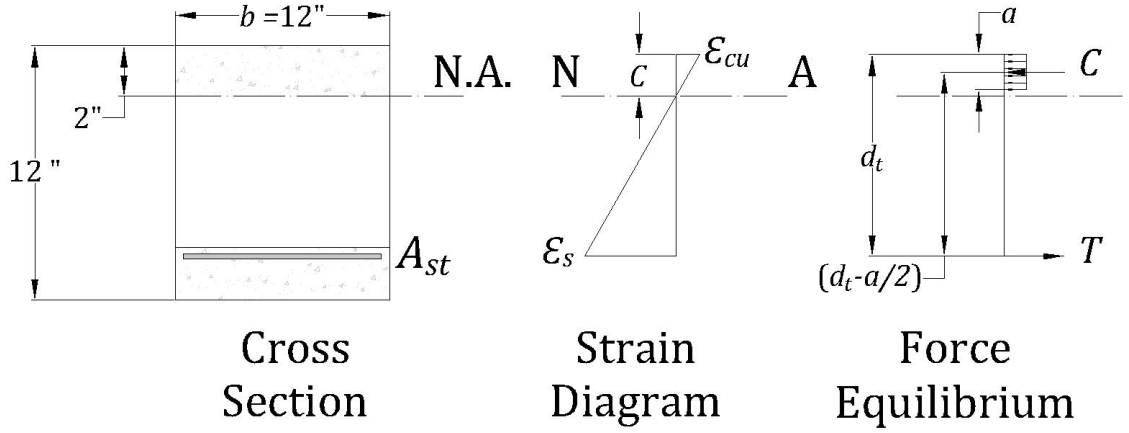

Figure (3.2): Strain variation and Force Equilibrium for cross section

Concrete Compressive strength: f'_c = 5000 psi gives α_1= 0.85 and β_1 = 0.85 (Per ACI 318-14)

Yield strength of steel: f_y = 56000 psi at ε_{sy} = 0.00206

No. of steel wires available in 1 foot of the width

= 4 wires (for 3.15" O.C. spacing or *x-direction*)

= 5 wires (for 2.9" O.C. spacing or *y-direction*)

Diameter of one steel wire, d_b = 3 mm = 0.1180 "

A_s for one steel wire = $\frac{\pi {d_b}^2}{4}$ = 0.0110 in^2

∴ Total tension steel area, $A_{st,x}$ = 0.0438 in^2 and $A_{st,y}$ = 0.0548 in^2

Modulus of Elasticity for steel = E_s = 29 x 10^6 psi

Another important assumption made for the analysis is that the strain in extreme concrete fiber has reached ultimate strain of ε_{cu} = 0.003 and steel has yielded. This condition is checked as shown below by estimating the actual strain in steel when the extreme concrete fiber strain (ε_{cu}) of 0.003 is reached. The nominal capacities for 12" thick slab are calculated

for each direction separately below. The capacity calculations for 10.5" thick slab are included in Appendix A.

i) *X-Direction*:

The depth of Whitney stress block is found as,

$$a = \beta_1 c = 0.85\ x\ 2 = 1.70"$$

The effective depth for tension steel is, d_t = (12 – 1.5 – 0.118/2) = 10.44"

The strain in steel wires can be found out by similar triangle method as follows,

$$\frac{\varepsilon_s}{(d_t - c)} = \frac{\varepsilon_{cu}}{c} \tag{3.1}$$

$$\frac{\varepsilon_s}{(10.4410 - 2.0000)} = \frac{0.0030}{2.0000}$$

$$\varepsilon_s = 0.0126 > \varepsilon_y = 0.0021$$

Hence, assumption that steel has yielded in tension is correct. The nominal moment capacity of the cross section in X-direction is given by:

$$M_{n,x} = A_{st,x} f_y (d_t - \frac{a}{2}) \text{ kip-in/ft} \tag{3.2}$$

$$M_{n,x} = 0.0548\ x\ 56\ x\ (10.4410 - \frac{1.7000}{2})$$

$$M_{n,x} = \text{ 23.5348 kip-in/ft =1.9604 kip-ft/ft (US Customary Units)}$$

$$M_{n,x} = \text{8.7203 kN-m /m (SI Units)}$$

If the assumption number v is violated and the contribution from the compression steel is considered, the nominal capacity calculated is greater than the capacity calculated in equation (3.2). Conservatively, lower capacity value is adopted for the failure load estimation. Similarly, the capacity is estimated for Y-direction as follows.

ii) *Y-Direction:*

The calculations till the steel strain estimation are similar to that of shown in equation (3.1). According to equation (3.1), the strain in steel is 0.0126 when the concrete strain in extreme fiber is reached to 0.003. The nominal capacity for the cross section in Y-direction can be predicted as follows,

$$M_{n,y} = A_{st,y} f_y (d_t - \frac{a}{2}) \text{ kip-in/ft} \quad (3.3)$$

$$M_{n,y} = 0.0438\ x\ 56\ x\ (10.4410 - \frac{1.7000}{2})$$

$$M_{n,y} = \text{ 29.4329 kip-in/ft =2.4527 kip-ft/ft (US Customary Units)}$$

$$M_{n,y} = 10.9101 \text{ kN-m /m (SI Units)}$$

3.3 PREDICTION OF FAILURE LOAD BY YIELD LINE METHOD

As explained in the earlier chapter, the two-way slab forms a yield line pattern forming failure mechanism when subjected to external loading. The test specimen considered for experiment, were square in shape and slab specimen A is evaluated in this section. Failure load for other slabs is evaluated in Appendix-B The possible yield line pattern for simply supported condition is shown in the Figure (3.3). The simple supported condition is evaluated here because the supporting Dywidag rods could possibly have subjected to slight rotation. Hence, the boundary condition could possibly not be as a complete fixed boundary.

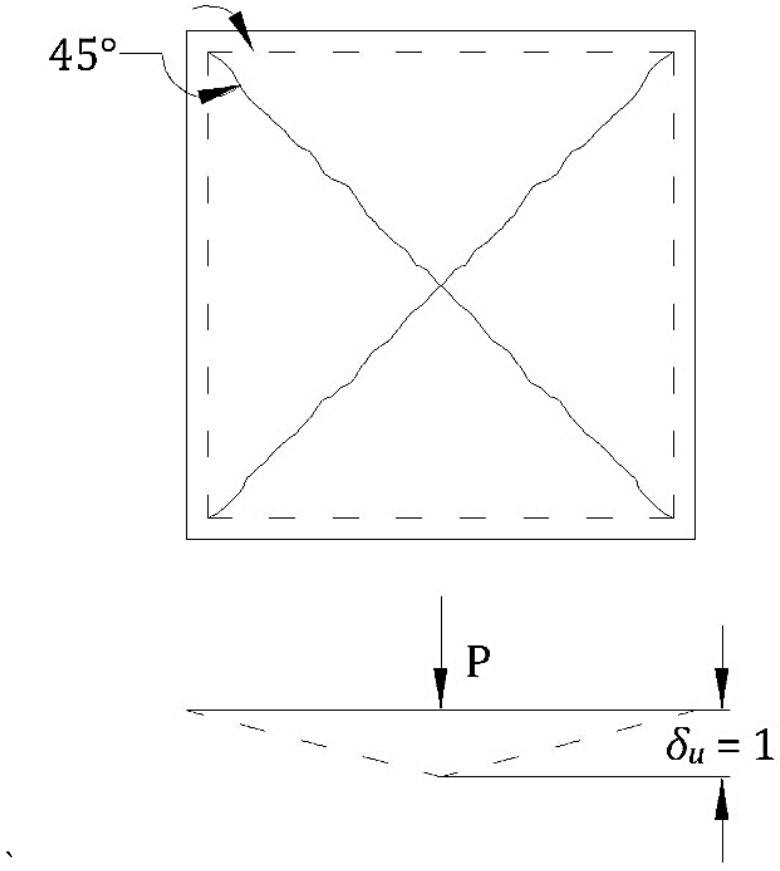

Figure (3.3): Yield Line Pattern and External Work Basis

The analysis using yield line pattern was carried out using the virtual work principle. When the yield line pattern is formed, the external moments and loads are said to be in equilibrium and an infinitesimal increase in load will cause slab to deflect further. The external work done by loads to cause small displacement must equal to the internal work done as slab parts rotate about the yield line to accommodate this deflection. The slab is given a virtual displacement, and corresponding rotations at yield lines can be estimated. By equilibrium of the internal and external work, the relation between applied loads and moment resistance of the slabs can be established [21].

The experiment condition is the square slab with concentrated loading at center of the slab. Figure (3.3) shows the basis of external work done by this load when the yield line forms. The virtual work done by external point load if it creates the unit displacement at center is given by,

$$W_{e1} = P_A \text{ x } \delta_u \tag{3.4}$$

The yield line divides slab into four triangular panels, which rotate about the yield line. Hence, the total external work done by the self-weight of the slab is given by,

$$W_{e2} = 4 \text{ x } w_D \frac{L_e^2}{4} \text{ x } \frac{\delta_u}{3} \tag{3.5}$$

The self-weight for 12" thick EPS concrete panel is 0.0606 kips/ft^2. The effective span L_e for the testing conditions is computed as ,

$$L_e = L - 2 \text{ x } (L_s)$$

$$L_e = 132" - 2 \text{ x } 9.625" = 112.75" = 9.39'$$

where, L_s = width of support plates = 9.625".

The self of slab will also contribute in the external work done and hence, the total external work done is given as,

$$W_e = W_{e1} + W_{e2} = P_A \text{ x } \delta u + w_D \frac{L_e^2}{2} \text{x } \frac{\delta_u}{3} = P_A \text{x} 1 - 4 \text{ x } 0.0606 \text{ x } \frac{9.39^2}{4} \text{x } \frac{1}{3}$$

$$W_e = (P_A - 1.78) \tag{3.6}$$

The yield line is skewed with respect to the direction of reinforcement and passes at diagonally at 45° with respect to the reinforcement. The combined resisting moment per unit length along the yield line is given as the algebraic sum shown [21].

$$M_\alpha = M_{n,x} \cos^2\alpha + M_{n,y} \sin^2\alpha \tag{3.7}$$

where, α is the inclination of yield line with respect to direction of reinforcement. Substituting α = 45° and values of $M_{n,x}$ and $M_{n,y}$ in equation (3.7),

$$M_\alpha = 1.9604 \text{ x } \cos^2 45 + 2.4527 \text{ x } \sin^2 45 = 2.21 \text{ kip-ft/ft}$$

The length of yield line is equal to twice of the diagonal of length of the slab and it is found as

$$L_y = 2 \text{ x } L_d = 2 \text{ x } 13.2877 \text{ ft} = 26.57 \text{ ft.}$$

When the displacement at center of the slab is unity, the rotation of the plastic hinge will be given as,

$$\theta = \frac{2}{6.6438} = 0.3010$$

Hence, total internal work done by the resisting moment along the yield line is,

$$W_i = L_y \text{ x } M_\alpha \text{ x } \theta = 26.5753 \text{ x } 2.2066 \text{ x } 0.3010 = 17.65$$

Equating W_e and W_i, one can obtain,

$$P_A = 19.43 \text{ kips (US Customary Units)}$$

$$\text{or, } P_A = 86.43 \text{ kN (SI Units)}$$

The slab will also be susceptible for two-way shear at the location of loading plate as there is a possibility that the loading plate itself may punch through small thickness of concrete before actually reaching the actual flexural load. Hence, it is important to estimate the punching shear capacity of the slab and compare it with failure load under flexure. Figure (3.4) shows critical section for punching for slab concrete layer. As the weak EPS core is embedded in between concrete layers, the loading plate is likely to punch through the concrete layer in contact. Hence, considering 2" (50.8 mm) thick concrete slab, punching shear capacity for slab is estimated per ACI 318-14 § 8.5.2 as shown in Figure (3.4),

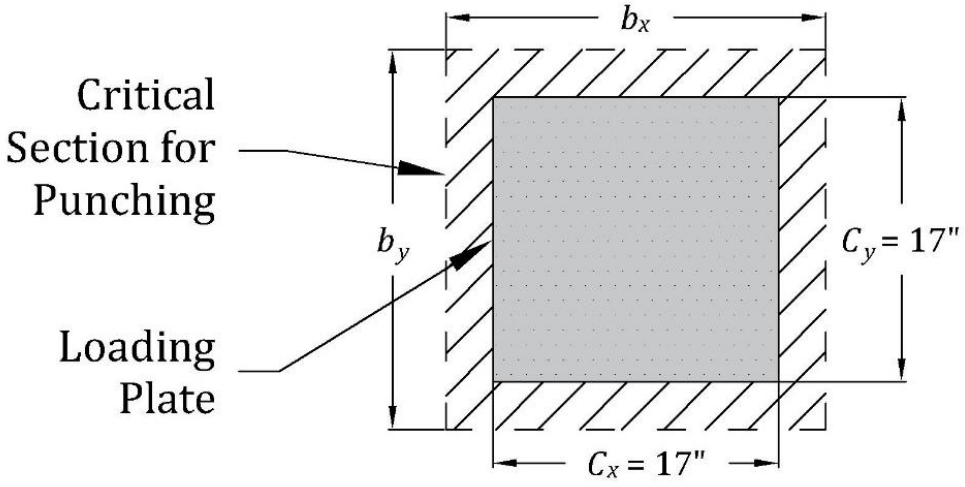

(1 inch = 25.4 mm)

Figure (3.4): Critical Perimeter for Punching

Slab effective depth (d_{eff}) = compression side concrete - half of bar diameter = 1.94'' (refer to Figure (3.4))

$b_x = C_x + d_{eff}$ = 18.94" and $b_y = C_y + d_{eff}$ = 18.94''

b_o = 2 x ($b_x + b_y$) = 75.76''

$A_c = b_o$ x d_{eff} = 147.06 in^2

α_s = 40 (assuming interior column condition)

$\beta_o = b_o / d$ = 37 and β_c = 1

ϕ = strength reduction factor = 0.75

Shear factor is considered minimum of the following:

S-Factor$_o$ = 2 + (α_s / β_o) = 3.08

S-Factor$_c$ = 2 + (4 / β_c) = 6

S-Factor$_{max}$ = 4

$$\text{S-Factor}_{\text{controlled}} = 3.08$$

$$\text{Controlled shear, } v_c = \text{S-Factor}_{\text{controlled}} \left(\sqrt{f_c'}\right) = 217.80 \text{ psi}$$

The ultimate punching shear strength is computed as,

$$\phi V_u = \phi v_c \text{ x } A_c = 0.75 \text{ x } 217.80 \text{ x } 147.06 = 24.03 \text{ kips (US Customary Units)}$$

$$\text{or, } \phi V_u = 106.89 \text{ kN (SI Units)}$$

It can be seen here that the flexural load capacity is smaller than the punching shear capacity for EPS concrete slabs. Hence, according to the theoretical analysis, the mode of failure shall be dominated by flexure and it can be confirmed from experimental results shown in Chapter 1. However, it shall also be confirmed with finite element analysis which is covered in the scope of next chapter.

Chapter 4

FINITE ELEMENT MODELLING OF TWO-WAY SANDWICH SLABS

4.1 INTRODUCTION

This chapter covers the evaluation of expanded polystyrene concrete composite slab for the two-way slab application using the finite element analysis (FEA). The work is based on the experimental work conducted on two-way concrete composite slab at University of California, Irvine (UCI). The objective of this section is to develop the load-displacement relationship using finite element analysis for determination of the suitability of sandwiched concrete composite slab for two-way application.

In this research, a detailed experimental analysis of three slab specimens of different dimensions and thickness was executed. The experimental results are discussed in this chapter later and are also compared with the results of finite element analysis. To improve the understanding of flexural behavior of sandwich panels, the finite element analysis (FEA) was undertaken using finite element program MARC. In the finite element model, the concrete and reinforcing steel are represented by separate materials and then are combined together with interaction between concrete and steel. The expanded polystyrene foam core has very low modulus of elasticity as compared to concrete and steel and hence the contribution from foam core to the flexural stiffness is very low. Therefore, the contribution of the EPS foam core was ignored in the numerical model. The results from finite element

analysis are compared with the experimental results and are validated using experimental data.

4.2 MATERIAL DEFINITIONS AND TYPE OF ELEMENTS

The finite element models were developed in order to predict the accurate behavior of sandwiched panels and the full scale models were developed using MARC. The full-scale model is the easiest way for modelling as it does not employ any scale down study [23]. The concrete and steel were modeled as isotropic materials which means that the material orientation does not affect mechanical properties [23]. The elastic properties of material are characterized by following parameters in finite element model,

E = Modulus of elasticity (ksi),

G = Shear Modulus (ksi) and

ν = Poisson's Ratio.

Using relation between Young's modulus, shear modulus and the Poisson's ratio, the shear modulus can be calculated as

$$G = \frac{E}{2(1+\nu)}$$

Using these properties, materials were defined separately in finite element model. However, to simulate actual behavior of EPS sandwiched panel, the actual properties of materials used shall be modeled in finite element model. The concrete and mortar possesses different behavior in compression and tension. It is very weak in tension and the behavior in compression is nonlinear i.e. the stress-strain relationship is not linear. Also, the stress strain relationship for steel is linear till elastic limit but it becomes non-linear after the yielding occurs. Hence, both materials were defined in finite element model using the nonlinear properties of the material.

In MARC®FE code, the nonlinear material properties are assigned by defining plasticity in material properties menu and it is shown in Figure (4.1). The material behavior was assumed to be as elastic-plastic isotropic in nature for analysis. The yield criterion can be defined by several methods and Von Mises stress criterion is used in this case as it defines better tensile behavior and smooth non-linear stress-strain relationship. The strain rate method was chosen as piecewise linear because of its advantages in computational efforts and plasticity definition. Following figure displays these definitions assigned in MARC.

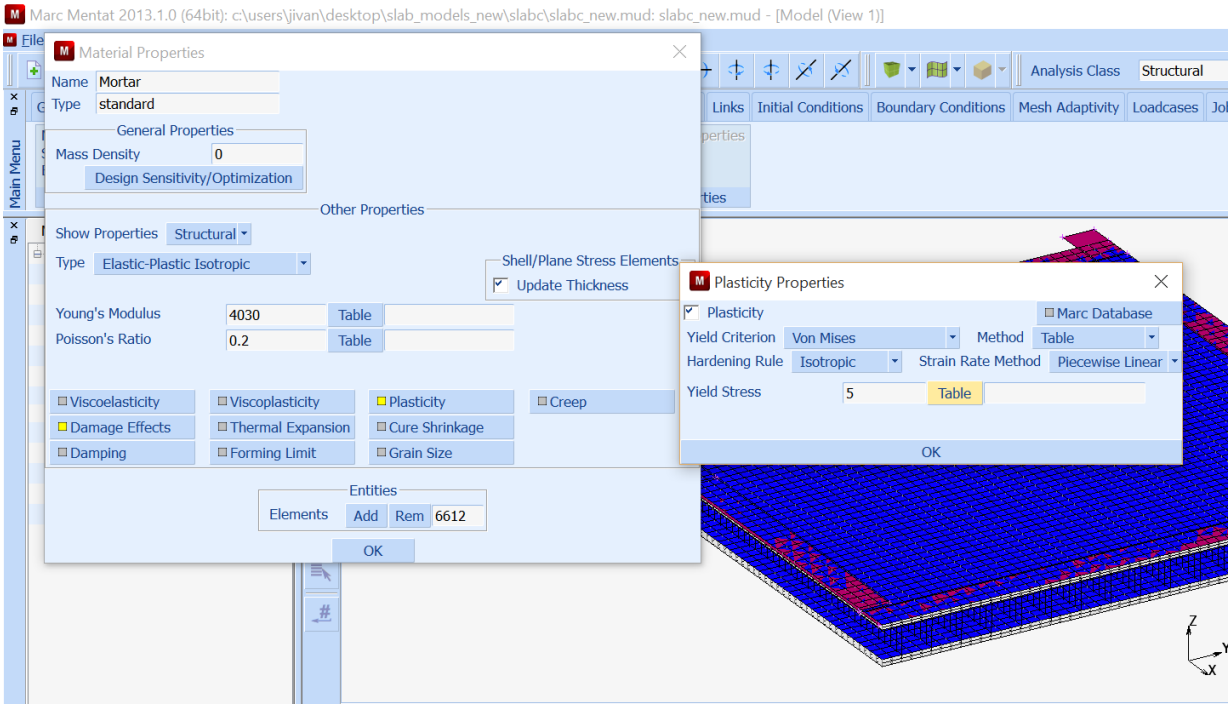

Figure (4.1): Material Properties of Concrete

Concrete cylinder were tested after 28 days to evaluate the characteristic compressive strength of concrete which yielded the approximate strength of 5 ksi (34.5 MPa). Hence, in compression, the characteristic strength of concrete (f'_c) was defined as 5 ksi (34.5 MPa) and modulus of elasticity and Poisson's ratio (ν_c) were assigned as 4030 ksi (27785.9 MPa) and 0.2 respectively. In MARC, failure properties are to be defined in damage effects. The ultimate compression strain of concrete was set equal to 0.004 as per ACI 318-14 code recommendations. The cracking properties of concrete are also defined in damage effects tab in MARC and the properties assigned are shown in Figure (4.2).

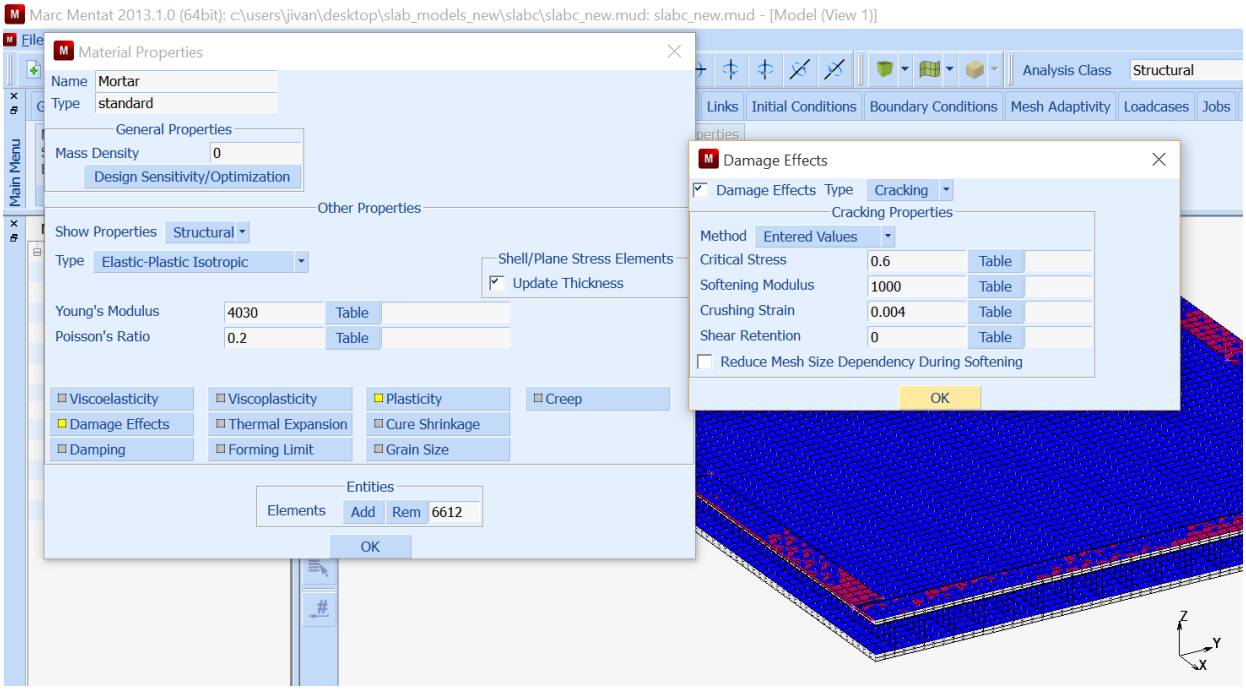

Figure (4.2): Damage effects for concrete defined in MARC

Elastic properties of steel were also defined in the similar fashion and are shown in Figure (4.3). The material properties assigned in MARC for each sample are summarized in following table.

Table (0.1): Material Properties

	Modulus of elasticity (E)	**Poisson's Ratio (v)**
Concrete	$5055.75\sqrt{f_c'}\ MPa$ ($57000\sqrt{f_c'}$ psi)	0.2
Steel	2×10^5 N/mm^2 (29×10^6 psi)	0.3

1 inch = 25.4 mm
1 ksi = 6.89 MPa

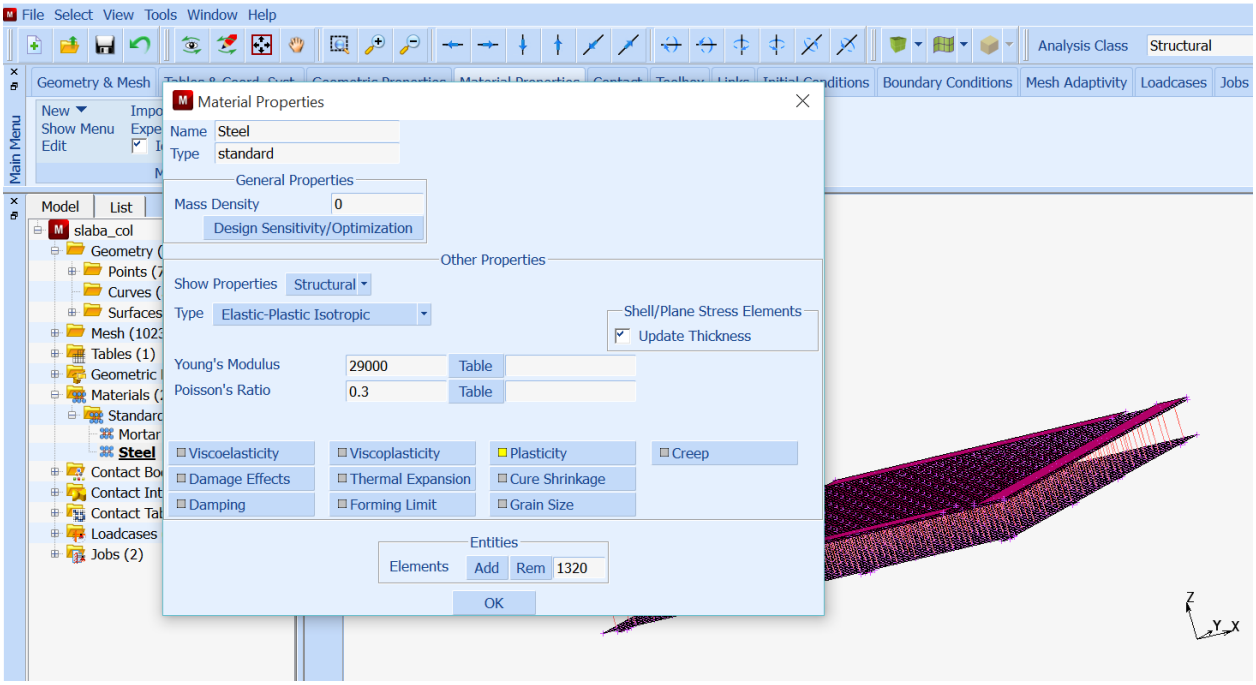

Figure (4.3): Material properties of Steel

Since steel reinforcement is used in concrete construction in the form of reinforcing bars or wire, it is not necessary to introduce the complexities of three-dimensional constitutive relations for steel. Axial force in the steel member will more than adequately represent the contribution to the physical deformation behavior of the overall member. Bending contribution for the overall member will automatically come through axial force of steel bar times the relevant arm from the neutral axis of overall member. So, there is no need to consider bending effects in the local coordinate system of reinforcement and hence, all steel wires were defined as 2 node line element.

The concrete elements are considered as plate elements with uniform thickness as the stress in concrete element would planar. Also, it consideration of concrete shell at plate element will help in reducing the computational efforts in analysis. Hence, the 4 node quadrilateral element was selected for defining concrete element.

4.3 MESH SIZE, LOADING AND BOUNDARY CONDITIONS

All of the EPS concrete slab panels tested in the experiment were modeled in MARC using the actual dimensions of the test specimens. This geometry was discretized using number of finite elements to simulate the experiment. As the mesh density increases, the accuracy of results calculated from finite element analysis also increase, but computational requirements are also increased. Hence, it is important to decide the mesh size before actually meshing the physical elements. The concrete element size was chosen as 3"x3" (*76.2 mm x 76.2 mm*) quadrilateral with 4 nodes at each corner and the steel elements were discretized with size of 2.25" (*57.15 mm*) long line element wit 2 nodes at end of each element. The nodes of steel elements were connected to the nodes of concrete quadrilateral elements. This mesh size provides fairly accurate results. Figure (4.4) shows the FE models for each slab specimen.

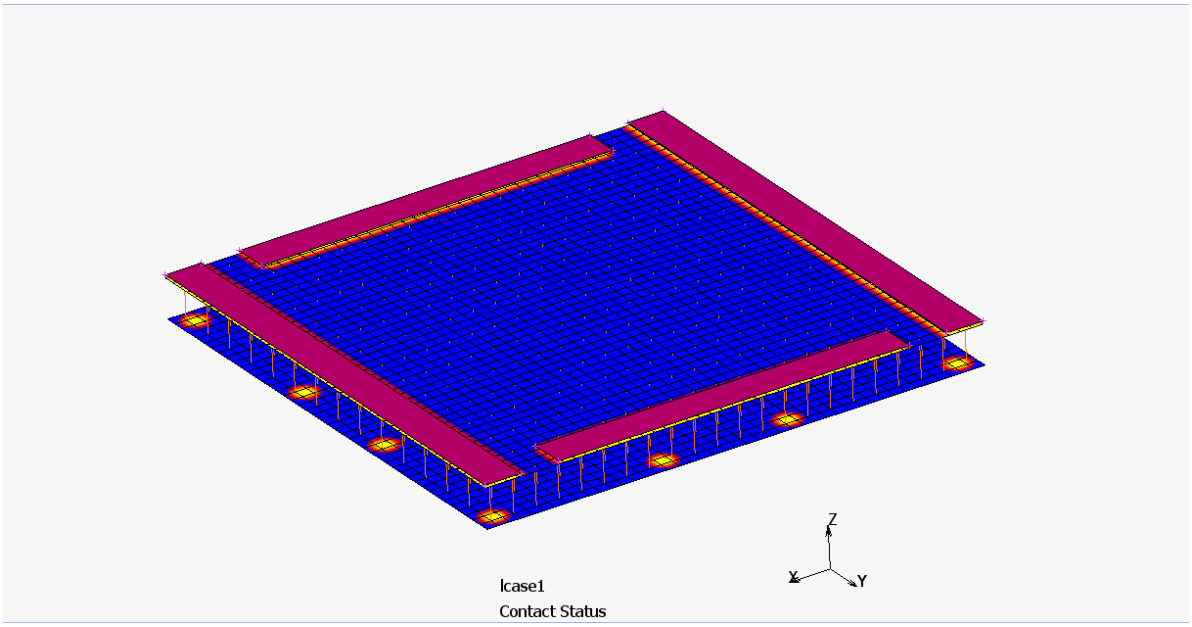

(a) Slab A Finite Element Model

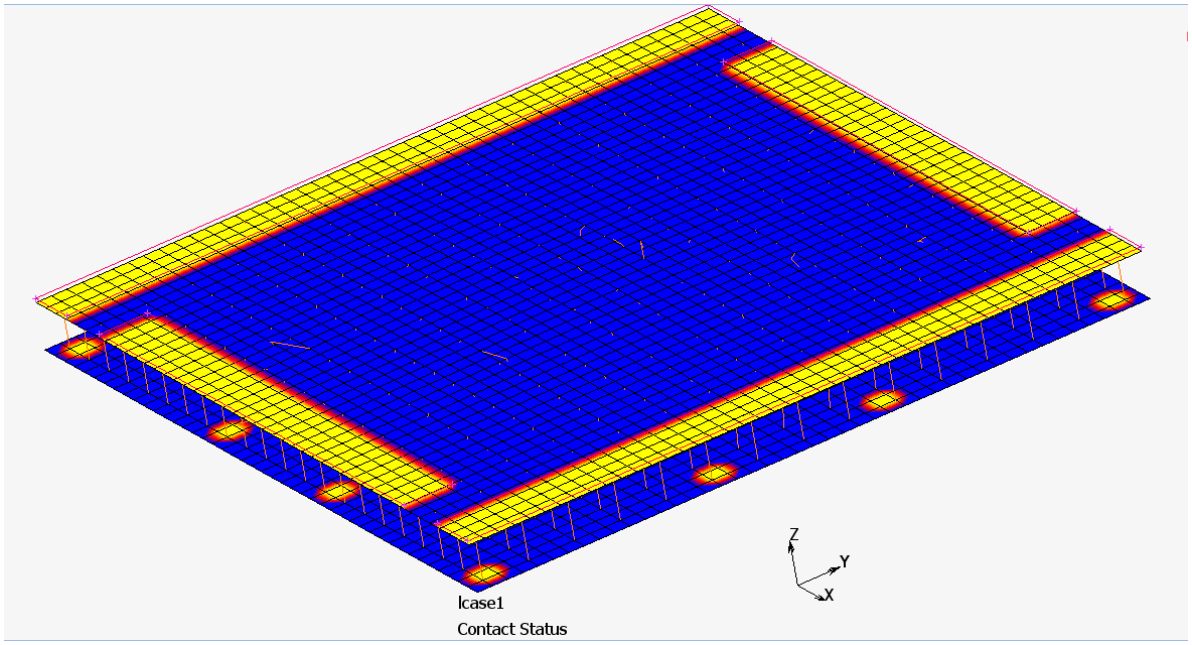

(b) Slab B Finite Element Model

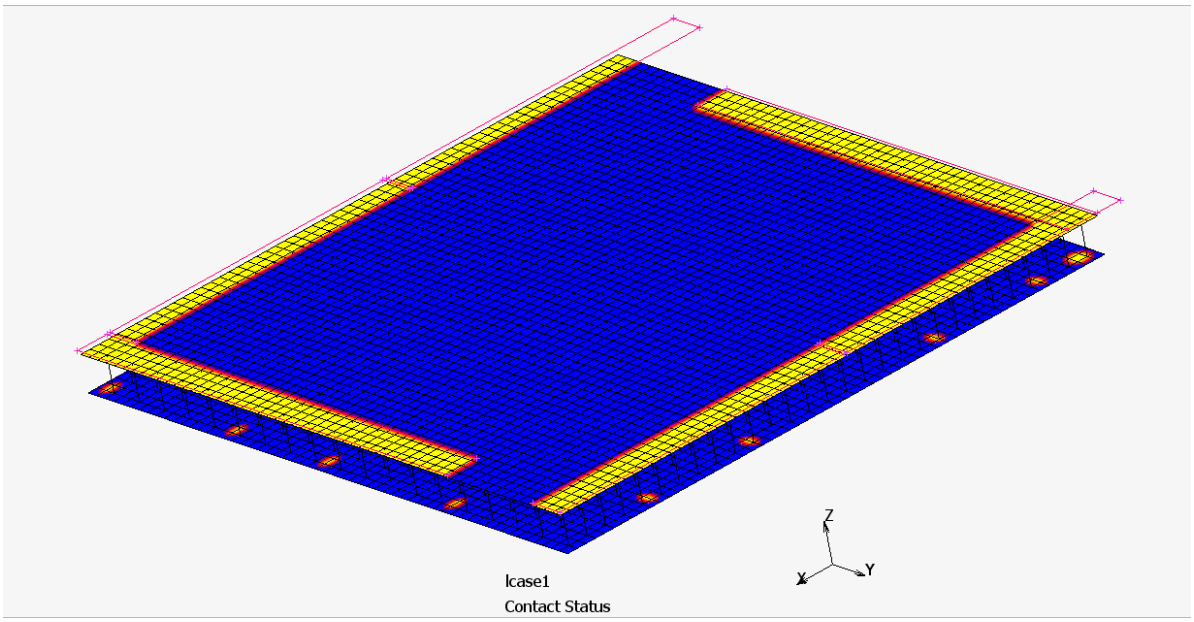

(c) Slab C Finite Element Model

Figure (4.4): Finite Element Models for Sandwich Slab Specimen

The accuracy of finite element analysis largely depends on appropriate selection of the boundary conditions defined in the model. In MARC FE code, the boundary conditions can be defined by assigning the conditions at nodes of the elements itself or by defining the contact interactions between the different surfaces. In the actual experiments, the steel plates were used to provide continuous fixed boundary at the edges of slabs. Hence, the boundary conditions were defined with the help of contact interaction definition between the steel support plates and concrete to simulate actual experiment conditions. MARC allows user to define contact type and assign this contact type for different bodies in model through contact table as shown in Figure (4.5).

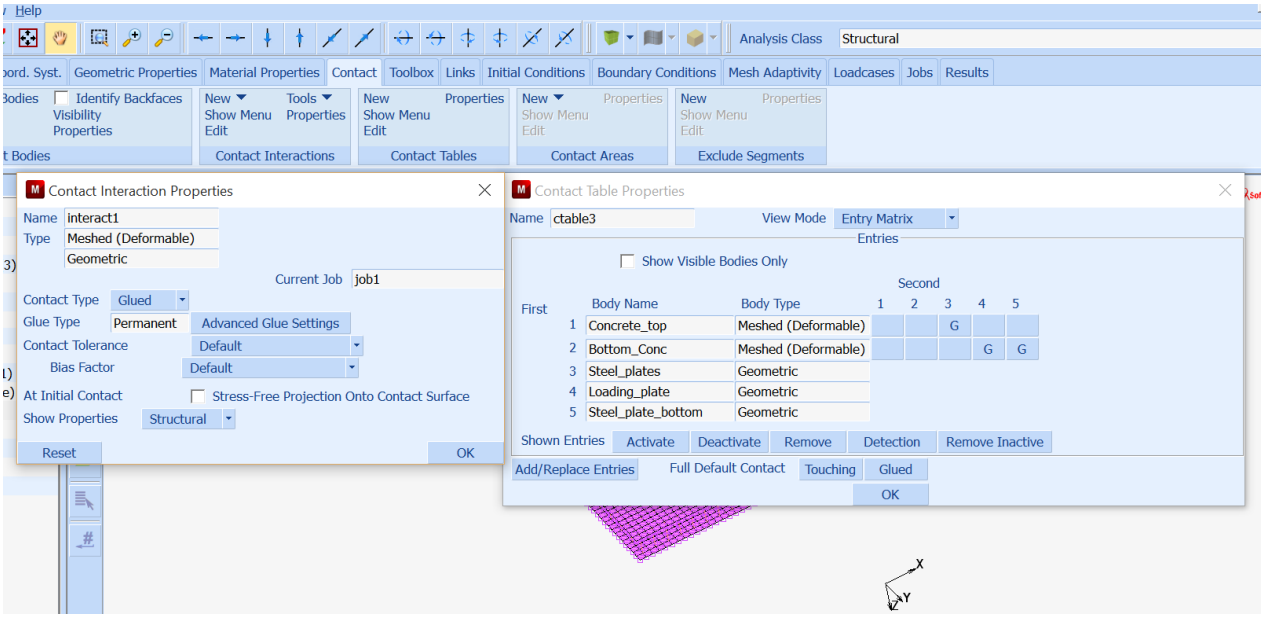

Figure (4.5): Boundary Conditions in MARC through Contact Interactions

The model analyses glued contact type as fixed boundary and automatically assigns conditions to nodes of adjacent finite elements. This option allows user in handling the boundary conditions imposed by the contact between two objects with ease with the finite element meshing. As shown in Figure (4.5), concrete elements are glued to steel plates at top and bottom which creates fixed boundary for concrete element. The contact interactions can be examined with the help of the contact status plot (in model plot option given in result tab) which is shown by yellow color in Figure (4.6). This indicates that the steel plate elements are permanently glued against the concrete elements and it will restrict the displacement of concrete elements creating the fixed boundary.

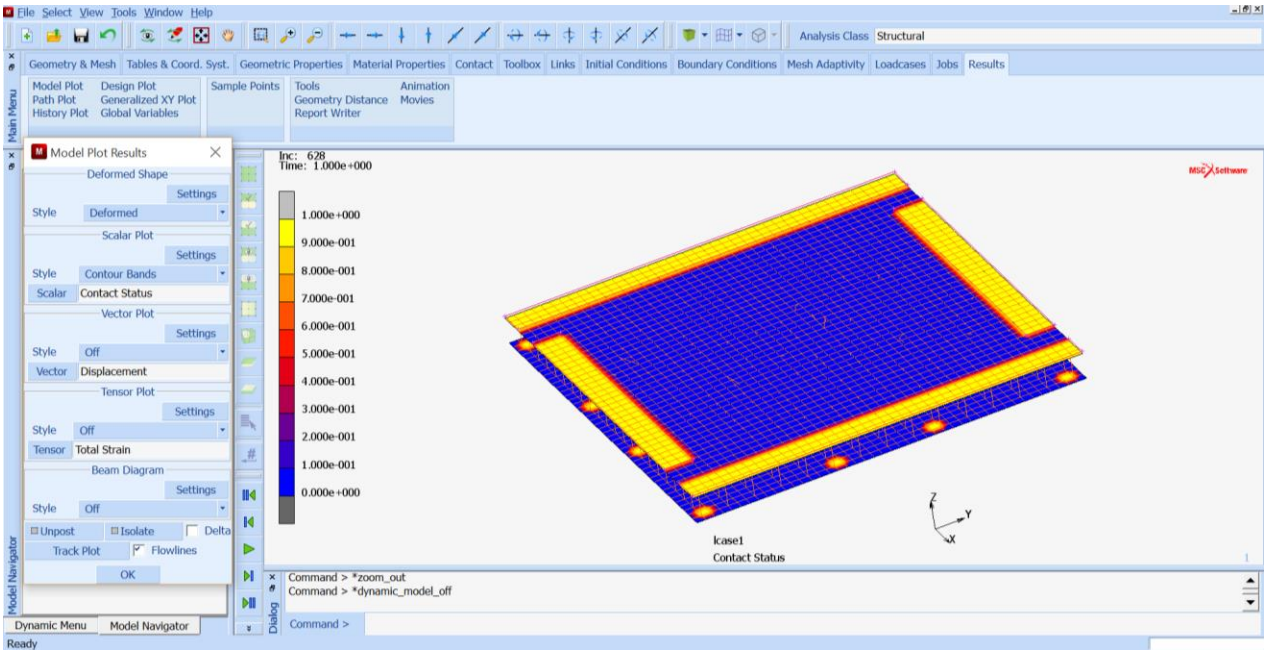

Figure (4.6): Contact Status in MARC

In the experiment, load was applied with the help of a 17" x 17" x 1" (*431.8 mm x 431.8 mm x 25.4 mm*) (*Length X Width X Thickness*) plate and a manually operated hydraulic actuator at the center of each slab specimen. This plate was modeled with its actual dimensions in the model and a static load case was assigned to the loading plate. In order to obtain the failure load for each specimen by finite element analysis, adaptive stepping load case was applied in finite element model uniform increment in load with uniform time step increment as shown in Figure (4.7). Each step has an increment of 5 units of load and maximum number of steps were set to a very high number so as to reach the failure state before final increment step is reached.

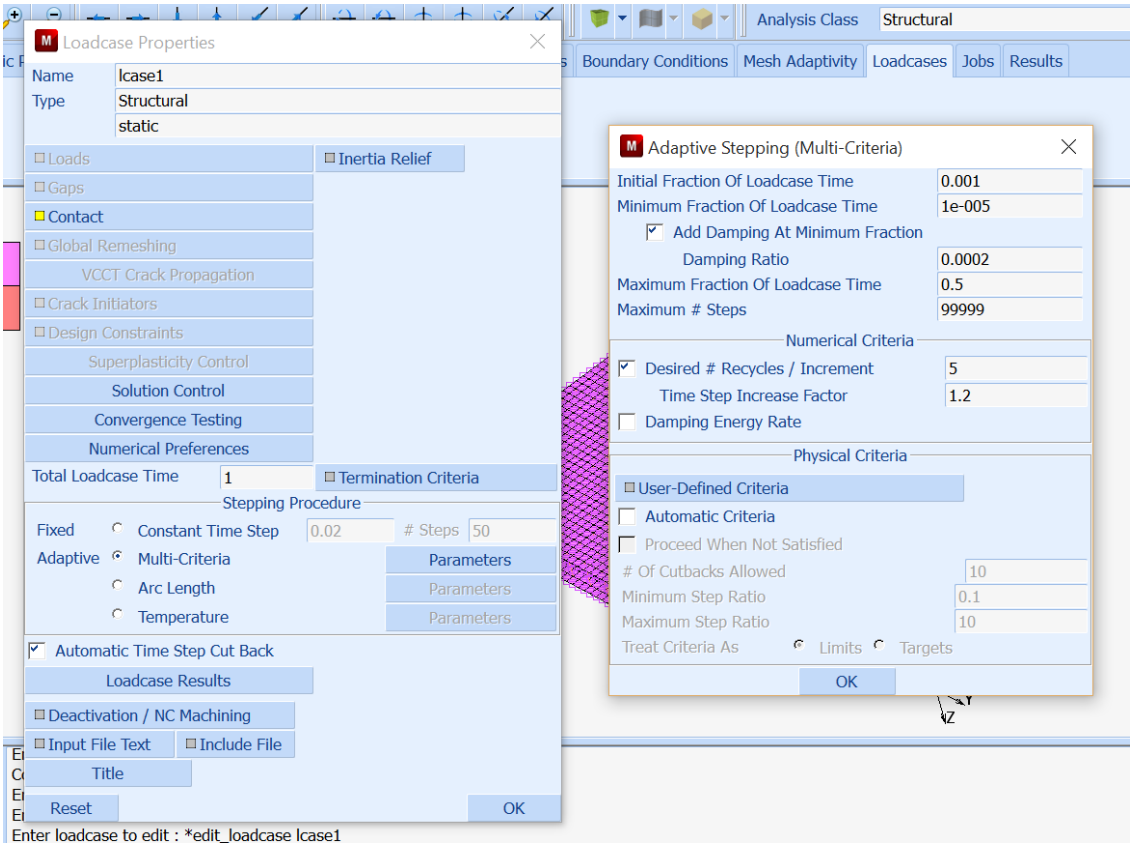

Figure (4.7): Load Case definition in MARC

4.4 ANALYSIS METHOD

As the response of a EPS concrete panels under consideration is not a linear function of the applied load, the methods of analysis used for the investigation of behavior of the sandwich panels are non-linear static analysis. Nonlinear behavior of the structure can be due to geometric nonlinearity, material nonlinearity, boundary nonlinearity or a combination of the three. In this study, the nonlinear behavior of the structure is due to material non-linearity of concrete and steel. Since, the modulus of elasticity of EPS is very small compared to concrete and steel, EPS is not included as a part of geometry.

In MARC, for initiating the analysis, the job has to be defined in different analysis classes in the program. For this study, analysis class is chosen as structural and a analysis job can be defined in it. As shown in Figure (4.8), a job can be defined to yield different set of results in form of analysis result tensors and scalars. For this research, large strain non-linear analysis option was chosen in analysis option tab as it allows to measure the change in dimensions of elements easily.

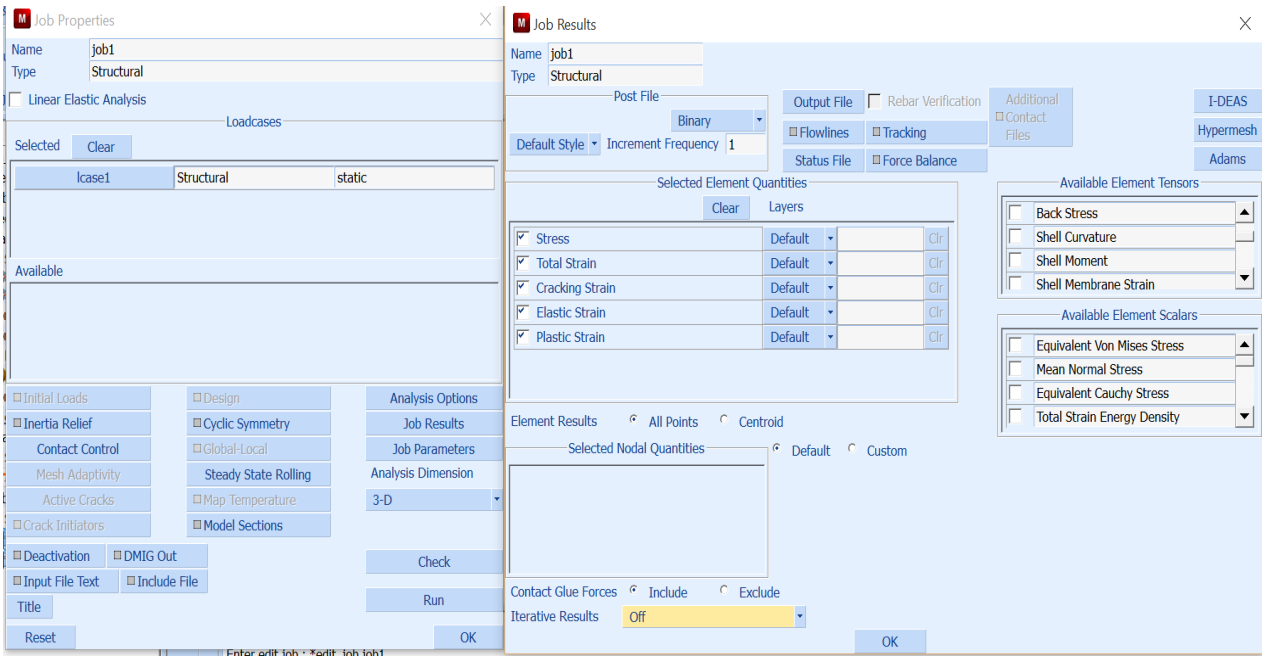

Figure (4.8): Analysis Job Definitions in MARC

4.5 FINITE ELEMENT RESULTS AND DISCUSSION

This section discusses the results obtained from three finite element models developed in MARC FE code for three different sandwich slab specimens evaluated in this study. Figure (4.9) shows typical deflected shape for the slab specimen which is obtained from the finite

element analysis. As mentioned earlier, the panel was modeled with full scale dimensions and a force was applied at the center of the slab with a square steel plate during testing. As expected, the maximum deflection occurred at the center of the slab. The deflection contours for the sandwich slab is shown in Figure (4.9). As shown in the figure, the dark blue color represents that there is displacement is approximately zero which is expected to occur near supports and bright yellow color indicates that the maximum displacement at the center of slab.

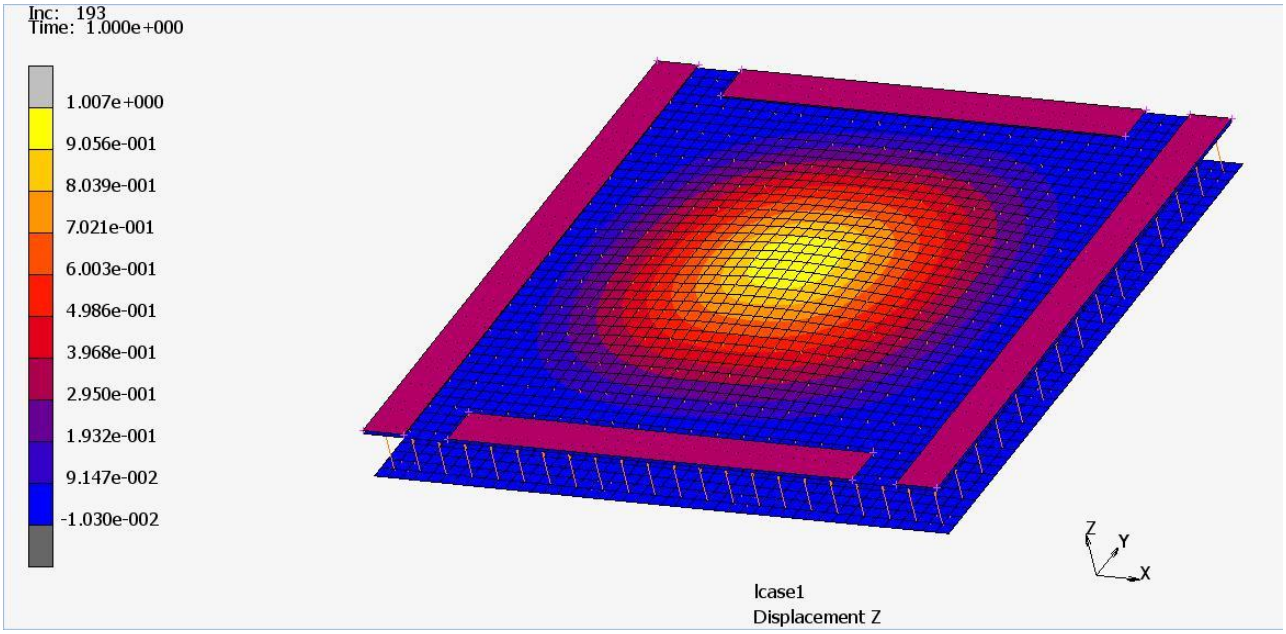

Figure (4.9): Simulated Deflected Shape of the Sandwich 3D Slab

As previously discussed, the finite element models were developed to simulate the sandwich slabs that were tested in the laboratory. From the finite element analysis, load vs. deflection relationships were obtained. The results were plotted in Excel® code and the numerical curve was compared to the full-scale experimental load-deflection curve (see Figures 4.10 to

4.12). As shown in these figures, an excellent correlation between experimental and numerical results is achieved.

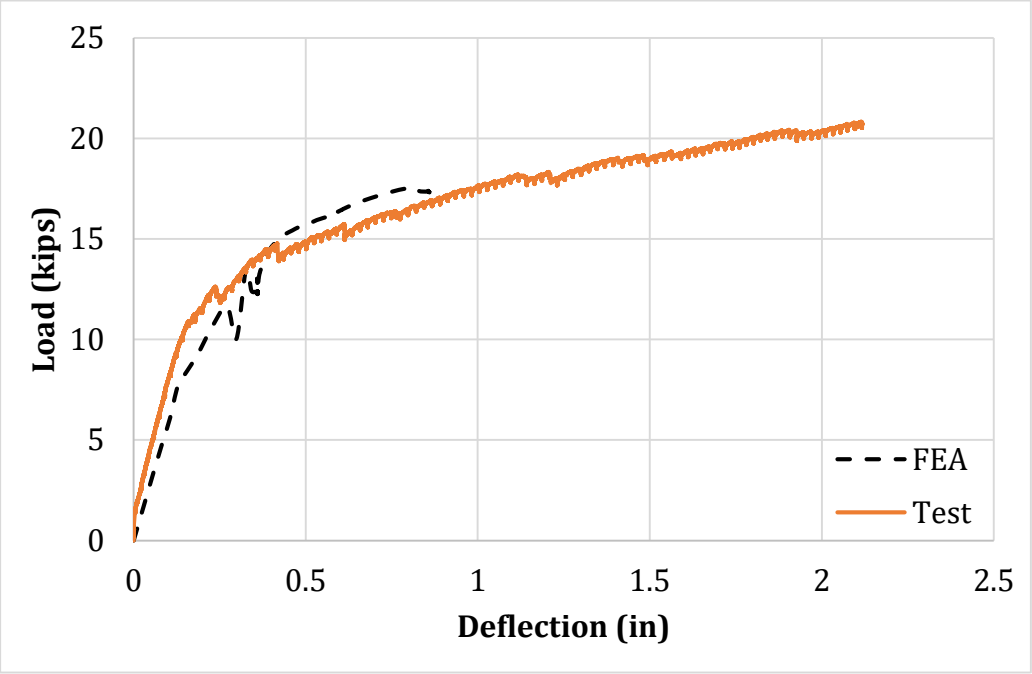

1 kip = 4.448 kN 1 inch = 25.4 mm

Figure (4.10): Comparison of Load Vs Deflection Curve for Slab A

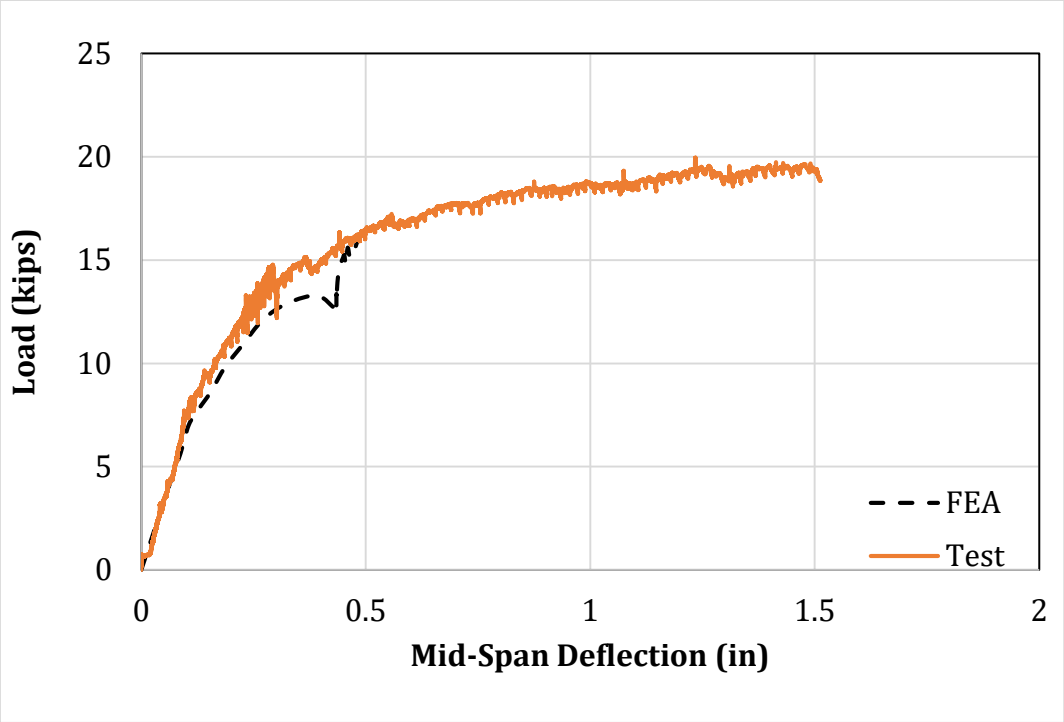

1 kip = 4.448 kN 1 inch = 25.4 mm

Figure (4.11): Comparison of Load Vs Deflection Curve for Slab B

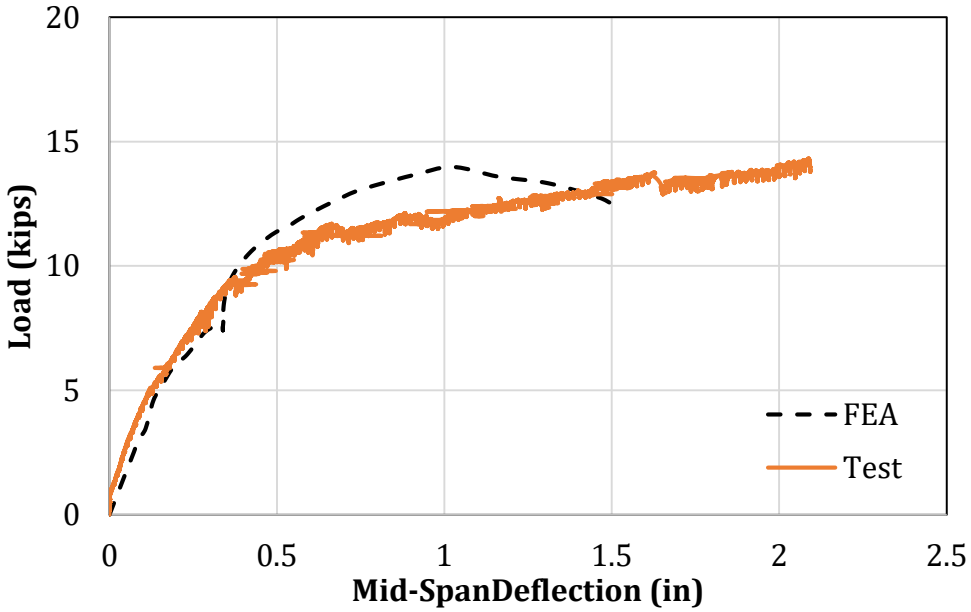

1 kip = 4.448 kN 1 inch = 25.4 mm

Figure (4.12): Comparison of Load Vs Deflection Curve for Slab C

The results can be compared in the non-dimesionalized entity which give better insight about the behavior of specimen with respect to its span. With the help of this, results of specimens with different dimensions can be compared easily. The load is non-dimesionalized with the help of modulus of elasticity of concrete and surface area of slab and deflection was non-dimesionalized by dividing deflection entities by span of the slab. Figures (4.13) shows comparison of non- dimesionalized load vs deflection curves for Slab Specimens "A", "B" and "C".

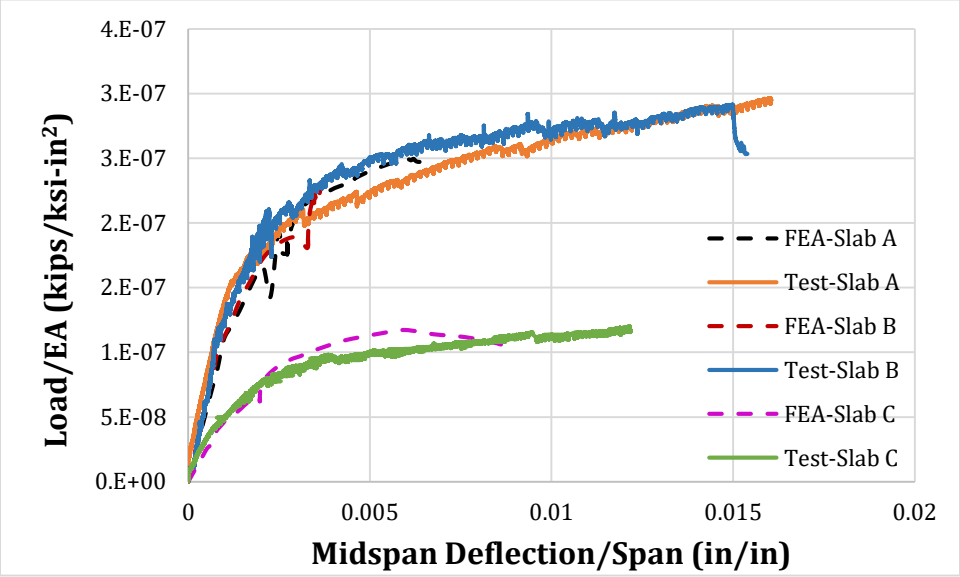

1 kip = 4.448 kN 1 inch = 25.4 mm

Figure (4.13): Comparison of Non-Dimesionalized Load Vs Deflection Curves for Slabs "A", "B" and "C".

In general, the results of finite element models were approximately close to the experimental measured results from the full-scale laboratory tests. However, there were slight differences between the experimental and numerically simulated results as shown in Figures (4.10) through (4.12). These differences in the values can be attributed to a number of reasons.

The first reason is based on the material properties which are used for modelling concrete and steel in MARC. These material properties defined in the model are as per the ACI 318-14 recommendations and values based on previous research work [23]. Therefore, the results of the finite element model could differ slightly depending upon the material properties used during the actual experimentation. In this study, conservative properties were assigned in finite element model because of which the difference between results might have been observed. The second reason for the deviation is that in the finite element model, contribution to the flexural stiffness from the EPS core was neglected. The expanded polystyrene foam may have some slight contribution to the stiffness of the slabs. This needs extensive finite element analysis with complex 3D modelling with exact properties of expanded polystyrene core. A third source of deviation is that in the FE model, all the edges of the slabs were assumed to be totally fixed, which in real tests may have some flexibility depending on the steel rod fixation and steel plate distribution along the edges of the tested slabs. Also and as one can notice from the load-deflection plots, the FE model did not predict the deflection at higher load levels due to the fact that the finite element model does not include the cracking of the mortar after the first crack occurs. This means that the finite element model did not have capability for determination of the crack propagation through mortar face. However, it can be confirmed that the model exhibits fairly close behavior as that of specimens experimentally tested.

Chapter 5

CONCLUSIONS AND RECOMMENDATIONS FOR FUTURE RESEARCH

This research project presented different analytical tools to predict the flexural behavior of two-way sandwich slabs with EPS foam core. The analytical procedures were verified through comparison with the results of full-scale experimental tests that were performed on three sandwich slabs with different dimensions and geometry. The analytical results correlate well with the full-scale experimental results.

5.1 CONCLUSIONS

The sandwich panelized slabs evaluated in this research demonstrated a relatively good composite behavior up to failure. The failure modes observed in the finite element models, as well as the experiments were mainly due to flexure.

Another objective of this research was to predict the load-carrying capacity of such sandwich two-way slabs subjected to out-of-plane flexural loads using analytical and finite element method. The numerical results were compared and confirmed with experimental analysis. Table (5.1) and Figure (5.1) present a summary of analytical, numerical and experimental maximum load carrying capacities of different sandwich slabs.

Table (5.1): Analytical and Experimental Maximum Load Carrying Capacity of Different Sandwich Slabs

Specimen	Experimental Load Capacity kips (in kN)	Analytical Load Capacity kips (in kN)	Finite Element Load Capacity kips (in kN)
Slab A	20.7 (92.1)	19.4 (86.4)	17.5 (77.8)
Slab B	20.5 (91.2)	16.7 (74.1)	16.3 (72.5)
Slab C	13.5 (60.1)	20.9 (93.1)	13.9 (61.8)

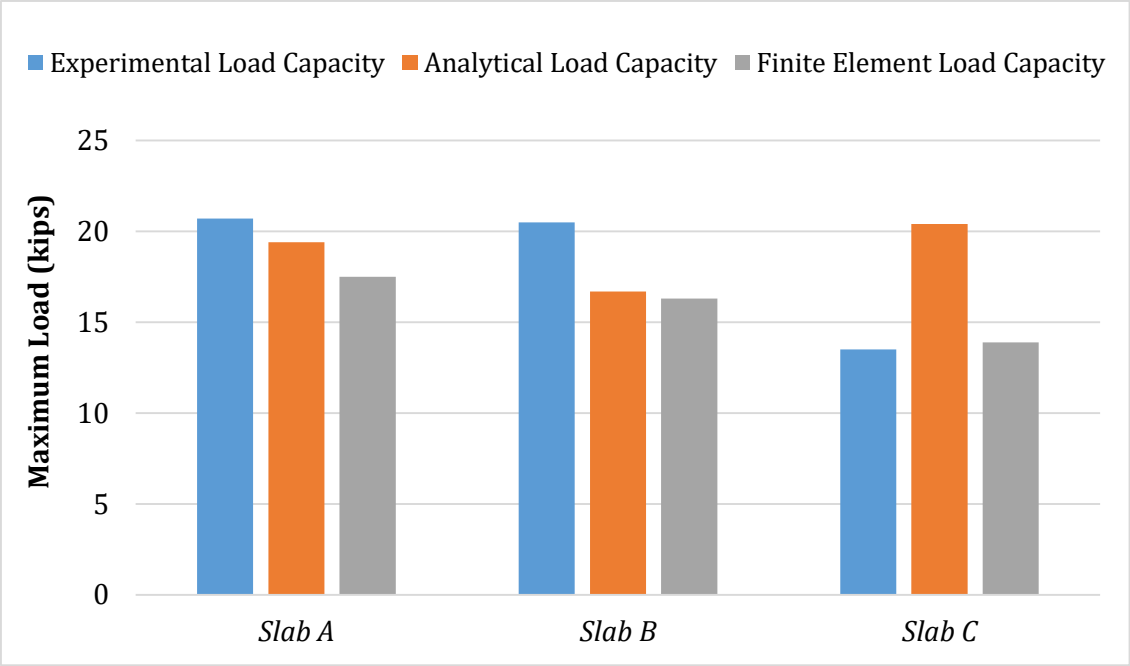

Figure (5.1): Comparison chart for Load Carrying Capacities

Figures (5.2) to (5.4) shows the crack pattern observed during the experiment for all of the specimen and Figures (5.5) to (5.6) shows the crack patterns predicted by finite element analysis for each of the slab specimen. It shows that the crack pattern as good correlation

between the assumed Yield Line pattern in Chapter 3 and crack pattern predicted by finite element analysis. The crack patterns observed are helpful in predicting the load path and failure pattern in future.

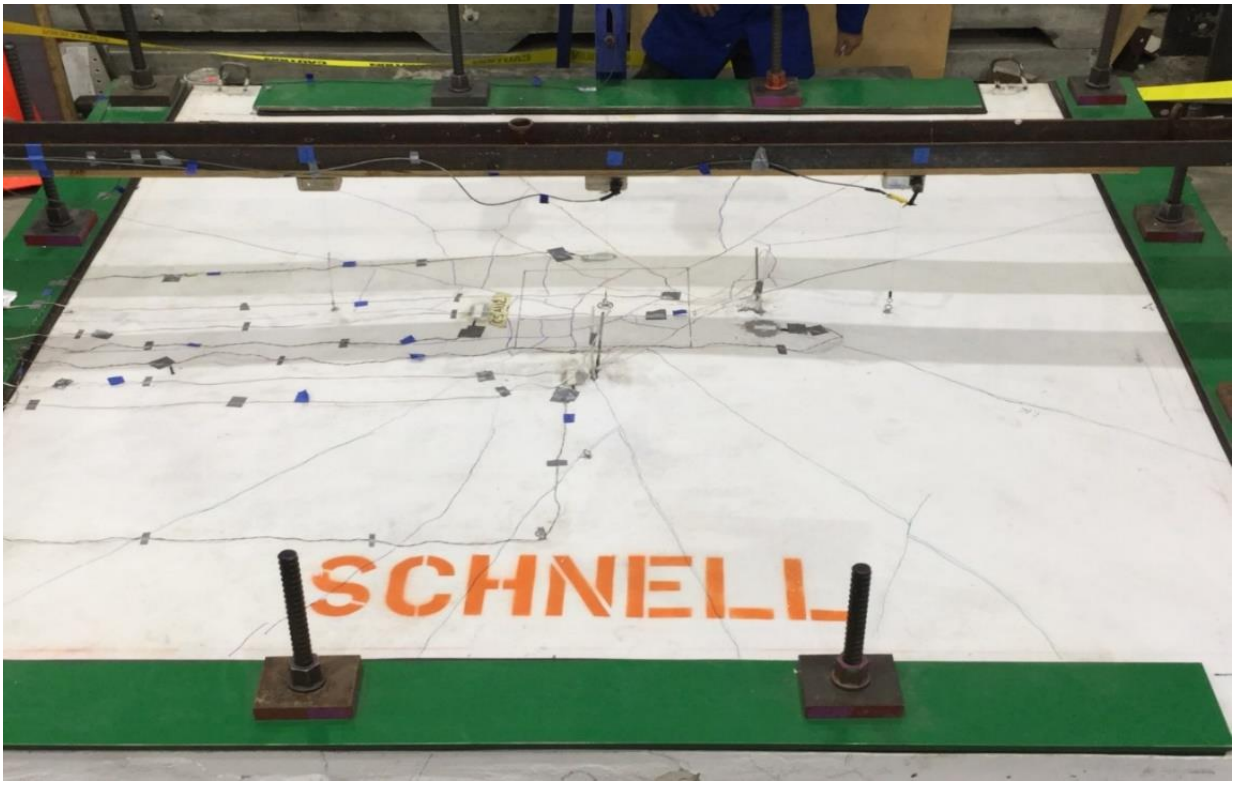

Figure (5.2): Crack Pattern for Slab Specimen "A"

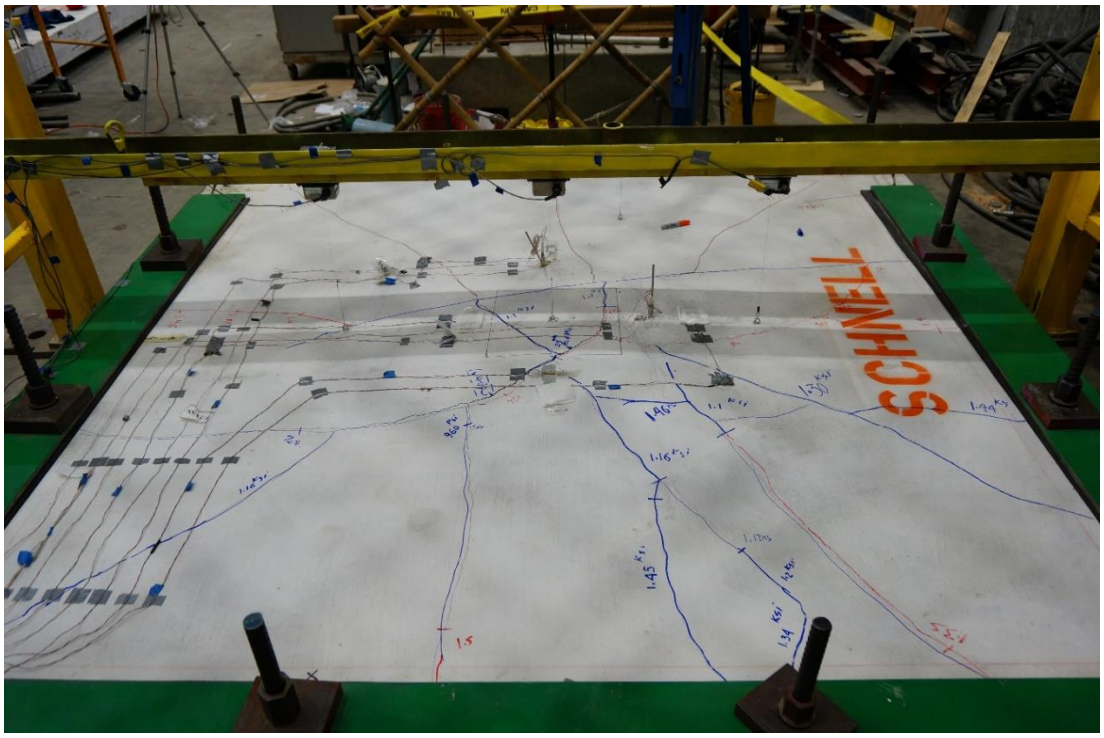

Figure (5.3): Crack Pattern for Slab Specimen "B"

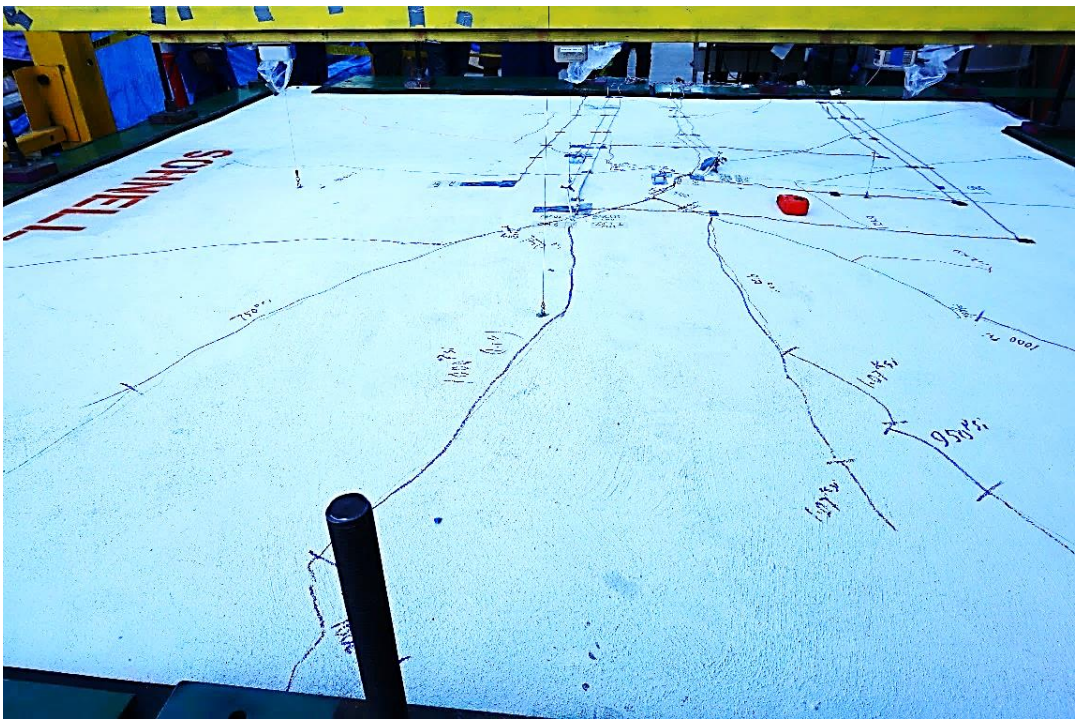

Figure (5.4): Crack Pattern for Slab Specimen "C"

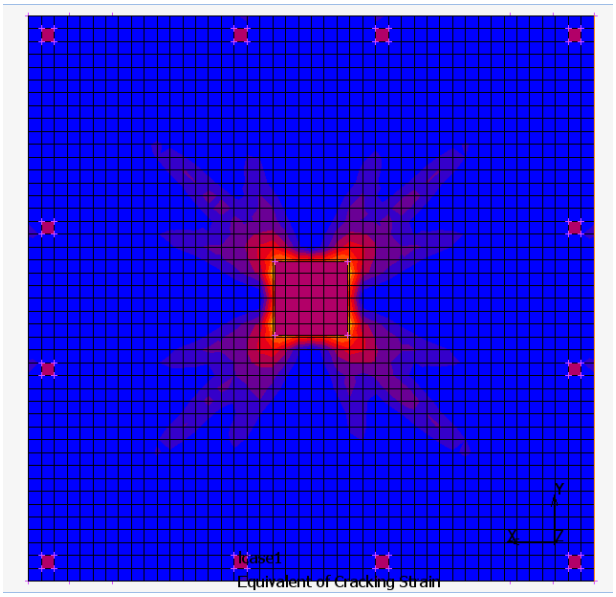

Figure (5.5): Crack Pattern for Slab Specimen "A" Predicted by FEA

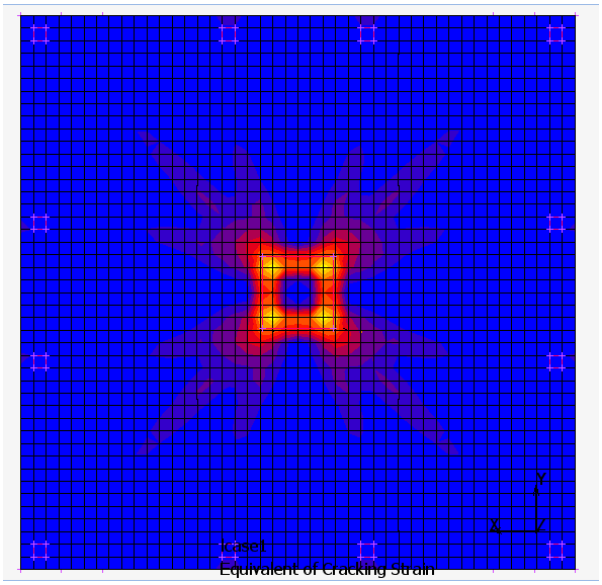

Figure (5.6): Crack Pattern for Slab Specimen "B" Predicted by FEA

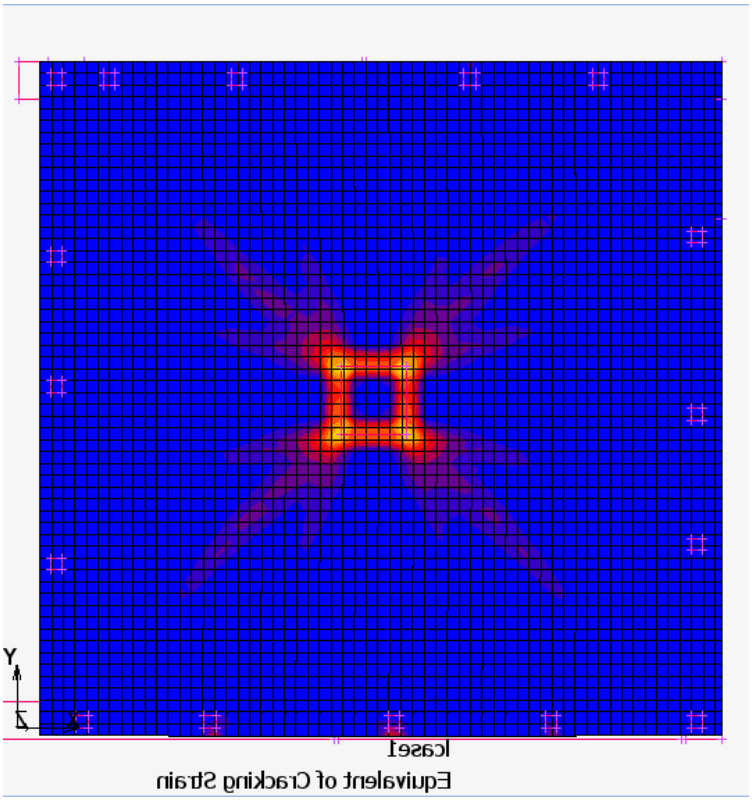

Figure (5.7): Crack Pattern for Slab Specimen "C" Predicted by FEA

As shown in Figure (5.1), one can confirm that the finite element method was able to predict the results which were closer to the actual experimental results. The theoretical analysis has significant deviation in the results as the assumptions which were made for theoretical analysis might not be always accurate. Also, the material nonlinearity is not considered in the theoretical analysis of the slabs which could a major reason for difference between the analytical and the experimental results. Furthermore, unlike finite element method, this method cannot be easily used for awkward shapes and geometry of the slabs. However, this method is very useful for quick load prediction without very complex and time consuming analysis.

5.2 RECOMMENDATIONS FOR FUTURE RESERCH

The applications of 3Dsandwich panels as an alternative method of construction offers several attractive unique features including its light-weight, superior thermal and acoustic insulation in addition to its cost effectiveness and rapid construction. However, due to the fact that these materials are included in the building codes creates difficulty for the structural engineers to widely use this system. For this reason, comprehensive qualifying tests are urgently needed to verify the structural characteristics of such systems and to develop design procedures that will assist engineers to design this non-conventional building system. For the past few years, UCI has been a frontier in this research area where several experimental and analytical studies have been performed on different 3D sandwich systems. This research has demonstrated that light-weight sandwich panels have a good potential for implementation as two-way structural floor/roof system. However, further research tasks are needed in order to understand the behavior of this system. The following are some of the recommendations for future research:

1. More tests need to be performed on large-scale slabs to evaluate the influence of different parameters such as boundary conditions, mortar compressive strength as well as the different geometry and arrangement of wires shear connectors,

2. Additional investigations on the behavior of sandwich slabs with different aspect ratios is needed to establish distribution factors in different directions,

3. As known in the literature, shear deformation of sandwich structures plays a major role on serviceability of such members, and hence research studies on shear deformation effect are recommended,

4. It is recommended to perform additional tests on sandwich slabs with supplemental hot-rolled reinforcements to decrease the thickness of such panels and to increase the economic advantages of such system,

5. The effect of two-way punching shear on these sandwich panels is also recommended,

6. Additional work on sandwich slabs with openings and the development of appropriate reinforcing details around these openings are required,

7. More research is recommended to evaluate the diaphragmatic behavior of the sandwiched in resisting lateral seismic loads,

8. Durability verification tests are essential to ensure the reliability and long-term behavior of the sandwich panels,

9. Due to the fact that these panels are considered as viscoelastic materials, more studies on the creep and recovery of such system is needed,

REFERENCES

[1] Surbhi Dadlani (2015); *"Experimental Evaluation of Two-Way Composite Floor Panels "*; Master's Thesis, University of California-Irvine, United States.

[2] James G. Macgregor et. al. (2005); *"Reinforced Concrete: Mechanics and Design"*; Pearson Prentice Hall, Pearson Education, Inc. Upper Saddle River, New Jersey 07458

[3] Ibrahim Mohammad Arman (2014); "*Analysis of two-way ribbed and waffle slabs with hidden beams"*; International Journal of Civil and Structural Engineering.

[4] Chu-Kia Wang and Charles G. Salmon (1985*); "Reinforced Concrete Design: Fourth Edition"*; Harper & Row Publication, New York.

[5] American Concrete Institute, ACI 318 "*Building Code Requirements for Structure Concrete and Commentary*", 2014.

[6] Ingerslev, A. (1923). *"The strength of rectangular plates*.'' J. Inst. Estruct. Eng. December

[7] Johansen, K. W. (1962); "*Yield-line theory";* Cement and Concrete Association, London.

[8] Johansen, K. W. (1972); "*Yield-line formulae for slabs"*; Cement and Concrete Association, London.

[9] Valentine Quintas (2003); "*Two main methods for Yield Line Analysis of Slabs"*; Journal of Engineering Mechanics, Vol. 129, No. 2, ©ASCE, ISSN 0733-9399/2003/2-223–231.

[10] Vázquez, M. (1994) ‘‘*Recocido simulado: un nuevo algoritmo para la optimacio´n de estructuras.*’’ PhD thesis, Universidad Polite´cnica de Madrid, Spain, Chap. 4.

[11] Hillerborg, A. (1996); “*Strip Method Design Handbook”*; E & FN Spon, Chapman & Hall Publications; London, UK

[12] Timoshenko, S.P and Gere, J.M. (1988); “*Theory of Elastic Stability”*; McGraw-Hill Publications, New York.

[13] Shu Jiangpeng et. al. (2014); Proc. of the 10th fib International PhD Symposium in Civil Engineering, Université Laval, Québec, Canada.

[14] Deaton J.B. (2005); “*A Finite element approach to reinforced concrete slab design”*; Master’s Thesis, Georgia Institute of Technology, United States.

[15] Zienkiewicz, O. C. and Cheung, Y. K., “*The Finite Element Method for Analysis of Elastic Isotropic and Orthotropic Slabs*,” Institution of Civil Engineers - Proceedings, vol. 28, pp. 471–488, August 1964.

[16] Wood, R. H., “*The Reinforcement of Slabs in Accordance with a Pre-Determined Field of Moments*,” Concrete, vol. 2, pp. 69–76, February 1968.

[17] Jofriet, J. C. and McNeice, G. M. (1971), “*Finite Element Analysis of Reinforced Concrete Slabs*,” ASCE Journal of the Structural Division, vol. 97.

[18] Famiyesin, O. O. R. and Hossain, K. M. A. (1998), “*Optimized Design Charts for Fully Restrained Slabs by FE Predictions*,” ASCE Journal of the Structural Division, vol. 124

[19] Zenkert, D (1995), “*An Introduction to Sandwich Construction*”, Engineering Materials Advisory Services, Cradley Heath, West Midlands, England.

[20] Bajracharya R.M. (2010) “*Structural Evaluation of Concrete-Expanded Polystyrene Sandwich Panels for Slab Applications*”; Master’s Thesis, University Southern

Queensland, Australia.

[21] Darwin D. et. al. (2015); "*Design of Concrete Structures*"; 15th edition; McGraw Hill Publications, New York.

[22] Brian Botello (2014); "*Experimental Evaluation of Sandwich Panels with Parallel Shear Connectors for Building Applications*"; Master's Thesis, University of California-Irvine, United States

[23] R. M. Bajracharya, W. P. Lokuge, W. Karunasena, K.T. Lau and A.S. Mosallam (2012); "*Structural evaluation of Concrete Expanded Polystyrene sandwich panels for slab applications*," Proceedings of the 22nd Australasian Conference on the Mechanics of Structures and Materials (ACMSM 2012): From Materials to Structures: Advancement through Innovation, 11-14 December, Sydney, Australia.

APPENDIX A

NOMINAL MOMENT CAPACITY OF 10.5" (267 mm) THICK SLAB SPECIMEN

The numerical calculations for the estimation of moment capacity of two-way slab with the thickness of 10.5" are discussed in this appendix. The calculations steps are similar to the 12" thick slab which are mentioned in Section 3.2 of Chapter 3. The assumptions utilized here are also same as those of adopted in Chapter 3 and the strain distribution for the section is shown in Figure (3.2).

Concrete Compressive strength: f'_c = 5000 psi gives α_1= 0.85 and β_1 = 0.85 (Per ACI 318-14 § 10.2.7)

Yield strength of steel: f_y = 56000 psi at ε_{sy} = 0.00206

No. of steel wires available in 1 foot of the width

= 4 wires (for 3.15" O.C. spacing or *x-direction*)

=5 wires (for 2.9" O.C. spacing or *y-direction*)

Diameter of one steel wire, d_b = 3 mm = 0.118 "

A_s for one steel wire = $\frac{\pi {d_b}^2}{4}$ = 0.011 in^2

∴ Total tension steel area, $A_{st,x}$ = 0.0438 in^2 and $A_{st,y}$ = 0.0548 in^2

Modulus of Elasticity for steel = E_s = 29 x 10^6 psi

Another important assumption made for the analysis is that the strain in extreme concrete fiber has reached ultimate strain of ε_{cu} = 0.003 and steel has yielded. This condition is checked as shown by estimating the actual strain in steel when the extreme concrete fiber strain (ε_{cu}) of 0.003 is reached. The nominal capacities for 10.5" thick slab are calculated for each direction separately.

iii) *X-Direction*:

The depth of Whitney stress block is found as,

$$a = \beta_1 c = 0.85\ x\ 2 = 1.70"$$

The effective depth for tension steel is, d_t = (10 – 1.5 – 0.118/2) = 8.44"

The strain in steel can be found out by similar triangle method as follows,

$$\frac{\varepsilon_s}{(d_t - c)} = \frac{\varepsilon_{cu}}{c} \qquad \text{(A.1)}$$

$$\frac{\varepsilon_s}{(8.4410 - 2.0000)} = \frac{0.003}{2.000}$$

Hence, assumption that steel has yielded in tension is correct. The nominal moment capacity of the cross section in X-direction is given by,

$$M_{n,x} = A_{st,x} f_y (d_t - \frac{a}{2}) \text{ kip-in/ft} \qquad \text{(A.2)}$$

$$M_{n,x} = 0.0438\ x\ 56\ x\ (8.94 - \frac{1.70}{2})$$

$$M_{n,x} = 19.84 \text{ kip-in/ft} = 1.65 \text{ kip-ft/ft (US Customary Units)}$$

$$M_{n,x} = 7.36 \text{ kN-m /m (SI Units)}$$

If the assumption number v is violated and the contribution from the compression steel is considered, the nominal capacity calculated is greater than the capacity calculated in equation (A.2). Conservatively, lower capacity value is adopted for the failure load estimation. Similarly, the capacity is estimated for Y-direction as follows.

iv) *Y-Direction:*

The calculations till the steel strain estimation are similar to that of shown in equation (A.1). The strain in steel is 0.0104 when the concrete strain in extreme fiber is reached to 0.003. The nominal capacity for the cross section in Y-direction can be predicted as follows,

$$M_{n,y} = A_{st,y} f_y (d_t - \frac{a}{2}) \text{ kip-in/ft}$$

$$M_{n,y} = 0.0548 \; x \; 56 \; x \; (8.94 - \frac{1.70}{2})$$

$$M_{n,y} = 24.83 \text{ kip-in/ft} = 2.07 \text{ kip-ft/ft (US Customary Units)}$$

$$M_{n,y} = 9.20 \text{ kN-m /m (SI Units)}$$

APPENDIX B

ESTIMATION OF LOAD CARRYING CAPACITY FOR SLABS "B" AND "C" USING YIELD LINE THEORY

1. ESTIMATION OF CAPACITY FOR SLAB "B"

The analysis using yield line pattern was carried out using the virtual work principle. The slab is given a virtual displacement, and corresponding rotations at yield lines can be estimated. By equilibrium of the internal and external work, the relation between applied loads and moment resistance of the slabs can be established.

The experiment condition is the square slab with concentrated loading at center of the slab. Figure (3.3) shows the basis of external work done by this load when the yield line forms. The virtual work done by external point load if it creates the unit displacement at center is given by,

$$W_{e1} = P_B \text{ x } \delta_u \tag{B.1}$$

The yield line divides slab into four triangular panels, which rotate about the yield line. Hence, the total external work done by the self-weight of the slab is given by,

$$W_{e2} = 4 \text{ x } w_D \frac{L_e^2}{4} \text{x } \frac{\delta_u}{3} \tag{B.2}$$

The self-weight for 10.5" thick sandwich slab is 0.0604 kips/ft^2. The effective span L_e for the testing conditions is computed as follows:

$$L_e = L - 2 \text{ x } (L_s)$$

$$L_e = 132" - 2 \text{ x } 9.625" = 112.75" = 9.3958'$$

where, L_s = width of support plates = 9.625".

The slab self-weight of contributes also to the external work done and hence, the total external work done is given as:

$$W_e = W_{e1} + W_{e2} = P_B \text{ x } \delta u + w_D \frac{L_e^2}{2} \text{x } \frac{\delta_u}{3} = P_B \text{x} 1 - 4 \text{ x } 0.0604 \text{ x } \frac{9.3958^2}{4} \text{x } \frac{1}{3}$$

$$W_e = (P_B - 1.7739) \quad \text{(B.3)}$$

The yield line is skewed with respect to the direction of reinforcement and passes at diagonally at 45° with respect to the reinforcement. The combined resisting moment per unit length along the yield line is given as the algebraic sum shown as follows [20].

$$M_\alpha = M_{n,x} \cos^2\alpha + M_{n,y} \sin^2\alpha \quad \text{(B.4)}$$

where, α is the inclination of yield line with respect to direction of reinforcement. Substituting α = 45° and values of $M_{n,x}$ and $M_{n,y}$ in equation (B.4),

$$M_\alpha = 1.6538 \text{ x } \cos^2 45 + 2.0691 \text{ x } \sin^2 45 = 1.8615 \text{ kip-ft/ft}$$

The length of yield line is equal to twice of the diagonal of length of the slab and it is found as

$$L_y = 2 \text{ x } L_d = 2 \text{ x } 13.2877 \text{ ft} = 26.5753 \text{ ft.}$$

When the displacement at center of the slab is unity, the rotation of the plastic hinge will be given as,

$$\theta = \frac{2}{6.6438} = 0.3010$$

Hence, total internal work done by the resisting moment along the yield line is,

$$W_i = L_y \text{ x } M_\alpha \text{ x } \theta = 26.5753 \text{ x } 1.8615 \text{ x } 0.3010 = 14.8904$$

Equating W_e and W_i, one can obtain,

$$P_B = 16.67 \text{ kips}$$

or, $P_B = 74.16$ kN

2. ESTIMATION OF CAPACITY FOR SLAB "C"

The virtual work done by external point load if it creates the unit displacement at center is given by,

$$W_{e1} = P_C \text{ x } \delta_u \qquad \text{(B.5)}$$

The yield line divides slab into four triangular panels, which rotate about the yield line. Hence, the total external work done by the self-weight of the slab is given by,

$$W_{e2} = 4 \text{ x } w_D \frac{L_e^2}{4} \text{x } \frac{\delta_u}{3} \qquad \text{(B.6)}$$

The self-weight for 12" thick EPS concrete panel is 0.0606 kips/ft^2. The effective span L_e for the testing conditions is computed as follows:

$$L_e = L - 2 \text{ x } (L_s)$$

$$L_e = 172" - 2 \text{ x } 9.625" = 152.75" = 12.7292'$$

where, L_s = width of support plates = 9.625".

The self of slab will also contribute in the external work done and hence, the total external work done is given as,

$$W_e = W_{e1} + W_{e2} = P_C \text{ x } \delta u + w_D \frac{L_e^2}{2} \text{x } \frac{\delta_u}{3} = P_C \text{x} 1 - 4 \text{ x } 0.0606 \text{ x } \frac{12.7292^2}{4} \text{x } \frac{1}{3}$$

$$W_e = (P_C - 3.2730) \quad \text{(B.7)}$$

The yield line is skewed with respect to the direction of reinforcement and passes at diagonally at 45° with respect to the reinforcement. The combined resisting moment per unit length along the yield line is given as the algebraic sum shown as follows [20].

$$M_\alpha = M_{n,x} \cos^2\alpha + M_{n,y} \sin^2\alpha \quad \text{(B.8)}$$

where, α is the inclination of yield line with respect to direction of reinforcement. Substituting α = 45° and values of $M_{n,x}$ and $M_{n,y}$ in equation (B.8),

$$M_\alpha = 1.9604 \text{ x } \cos^2 45 + 2.4527 \text{ x } \sin^2 45 = 2.2066 \text{ kip-ft/ft}$$

The length of yield line is equal to twice of the diagonal of length of the slab and it is found as

$$L_y = 2 \text{ x } L_d = 2 \text{ x } 18.0018 \text{ ft} = 36.0036 \text{ ft.}$$

When the displacement at center of the slab is unity, the rotation of the plastic hinge will be given as,

$$\theta = \frac{2}{9.0009} = 0.2222$$

Hence, total internal work done by the resisting moment along the yield line is,

$$W_i = L_y \text{ x } M_\alpha \text{ x } \theta = 36.0036 \text{ x } 2.2066 \text{ x } 0.2222 = 17.6528$$

Equating W_e and W_i, one can obtain,

$$P_C = 20.93 \text{ kips}$$

or, $P_C = 93.11$ kN